University of Groningen

Extracellular vesicles derived from fat-laden hepatocytes undergoing chemical hypoxia promote a pro-fibrotic phenotype in hepatic stellate cells

Hernández, Alejandra; Reyes, Daniela; Geng, Yana; Arab, Juan Pablo; Cabrera, Daniel; Sepulveda, Rolando; Solis, Nancy; Buist-Homan, Manon; Arrese, Marco; Moshage, Han

IMPORTANT NOTE: You are advised to consult the publisher's version (publisher's PDF) if you wish to cite from it. Please check the document version below.

Document Version
Publisher's PDF, also known as Version of record

Publication date:
2020

[Link to publication in University of Groningen/UMCG research database](#)
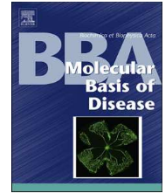
Extracellular vesicles derived from fat-laden hepatocytes undergoing chemical hypoxia promote a pro-fibrotic phenotype in hepatic stellate cells

Alejandra Hernández[a,b], Daniela Reyes[a], Yana Geng[b], Juan Pablo Arab[a,c], Daniel Cabrera[a,d,e], Rolando Sepulveda[a], Nancy Solis[a], Manon Buist-Homan[b], Marco Arrese[a,c], Han Moshage[b,*]

[a] *Departamento de Gastroenterología, Escuela de Medicina, Pontificia Universidad Católica de Chile, Santiago, Chile*
[b] *Department of Gastroenterology and Hepatology, University of Groningen, University Medical Center Groningen, Groningen, the Netherlands*
[c] *Centro de Envejecimiento y Regeneración (CARE), Departamento de Biología Celular y Molecular, Facultad de Ciencias Biológicas Pontificia Universidad Católica de Chile, Santiago, Chile*
[d] *Facultad de Ciencias Médicas, Universidad Bernardo O Higgins, Santiago, Chile*
[e] *Departamento de Ciencias Químicas y Biológicas, Facultad de Salud, Universidad Bernardo O Higgins, Santiago, Chile*

ARTICLE INFO

ABSTRACT

Background: The transition from steatosis to non-alcoholic steatohepatitis (NASH) is a key issue in non-alcoholic fatty liver disease (NAFLD). Observations in patients with obstructive sleep apnea syndrome (OSAS) suggest that hypoxia contributes to progression to NASH and liver fibrosis, and the release of extracellular vesicles (EVs) by injured hepatocytes has been implicated in NAFLD progression.
Aim: To evaluate the effects of hypoxia on hepatic pro-fibrotic response and EV release in experimental NAFLD and to assess cellular crosstalk between hepatocytes and human hepatic stellate cells (LX-2).
Methods: HepG2 cells were treated with fatty acids and subjected to chemically induced hypoxia using the hypoxia-inducible factor 1 alpha (HIF-1α) stabilizer cobalt chloride (CoCl2). Lipid droplets, oxidative stress, apoptosis and pro-inflammatory and pro-fibrotic-associated genes were assessed. EVs were isolated by ultracentrifugation. LX-2 cells were treated with EVs from hepatocytes. The CDAA-fed mouse model was used to assess the effects of intermittent hypoxia (IH) in experimental NASH.
Results: Chemical hypoxia increased steatosis, oxidative stress, apoptosis and pro-inflammatory and pro-fibrotic gene expressions in fat-laden HepG2 cells. Chemical hypoxia also increased the release of EVs from HepG2 cells. Treatment of LX2 cells with EVs from fat-laden HepG2 cells undergoing chemical hypoxia increased expression pro-fibrotic markers. CDAA-fed animals exposed to IH exhibited increased portal inflammation and fibrosis that correlated with an increase in circulating EVs.
Conclusion: Chemical hypoxia promotes hepatocellular damage and pro-inflammatory and pro-fibrotic signaling in steatotic hepatocytes both *in vitro* and *in vivo*. EVs from fat-laden hepatocytes undergoing chemical hypoxia evoke pro-fibrotic responses in LX-2 cells.

1. Introduction

Non-alcoholic fatty liver disease (NAFLD) is currently the most common liver disease and a major global health problem [1,2]. NAFLD is characterized by fat accumulation in the liver, which may progress to steatohepatitis, cirrhosis and determine liver-related morbidity and mortality [3]. Recent evidence suggests that the accumulation of saturated fatty acids (FFAs) contribute to the occurrence of lipotoxicity and

View PDF

Fig. 1. Chemical hypoxia stabilizes HIF-1α in liver cells. HepG2 cells were incubated for 24 h with oleic acid and palmitic acid 2:1 (FFA) in the presence or absence of CoCl₂ 200 μmol/l. Protein levels of HIF-1α were determined by Western blotting as described in Material and Methods. α-tubulin was used as a loading control. Data are shown as the mean ± SEM ($n \geq 3$) **** indicates $P < 0.001$.
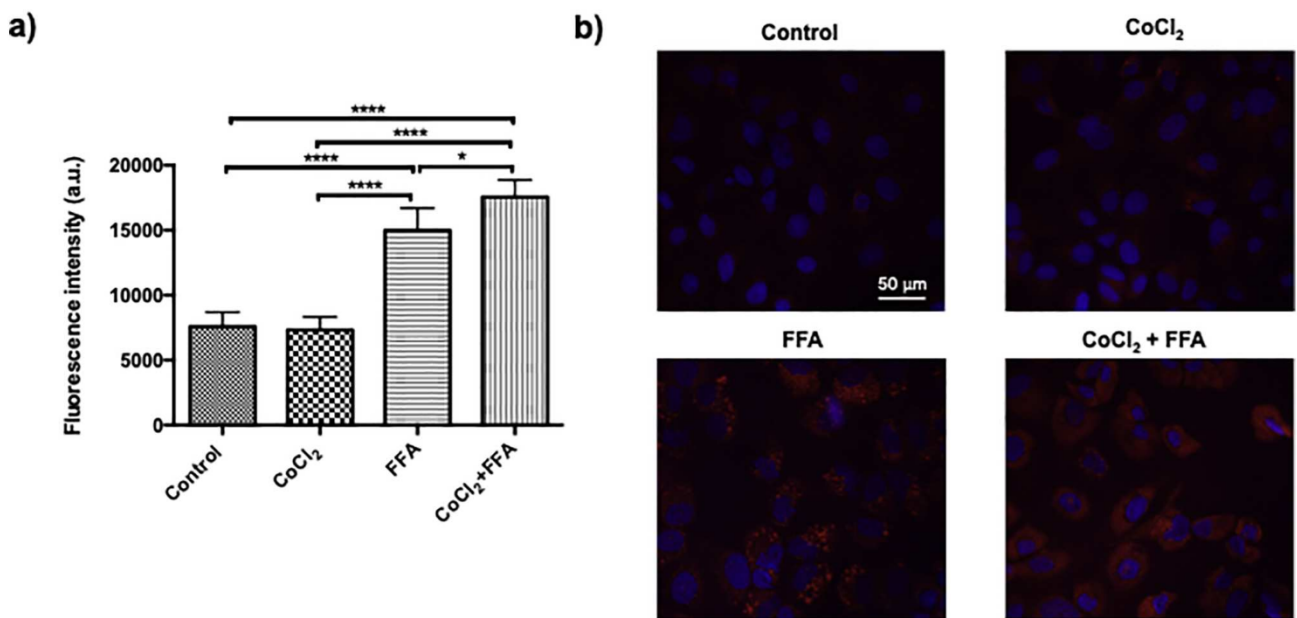
Fig. 2. Chemical hypoxia aggravates FFA-induced steatosis *in vitro*. HepG2 cells were incubated for 24 h with oleic acid and palmitic acid 2:1 (FFA) in the presence or absence of CoCl₂ 200 μmol/l. Lipid droplet content was assessed by the fluorescence intensity (a) of Nile Red stained images (b) as described in Material and Methods. Data are shown as the mean ± SEM (n ≥ 3) * indicates $P < 0.05$; **** indicates $P < 0.001$.

can trigger hepatic inflammation and an abnormal wound-healing re-
sponse and fibrogenesis leading to non-alcoholic steatohepatitis
... liver fibrosis and ultimately to

cirrhosis [3–5].
    Why some patients with NAFLD progress to NASH and advanced
fibrosis more rapidly and severely than others remains unclear [5].

Fig. 3. Chemical hypoxia increases the production of reactive oxygen species in steatotic HepG2 cells. HepG2 cells were incubated for 24 h with oleic acid and palmitic acid 2:1 (FFA) in the presence or absence of $CoCl_2$ 200 µmol/l. Reactive oxygen species (ROS) were measured as described in Material and Methods. Data a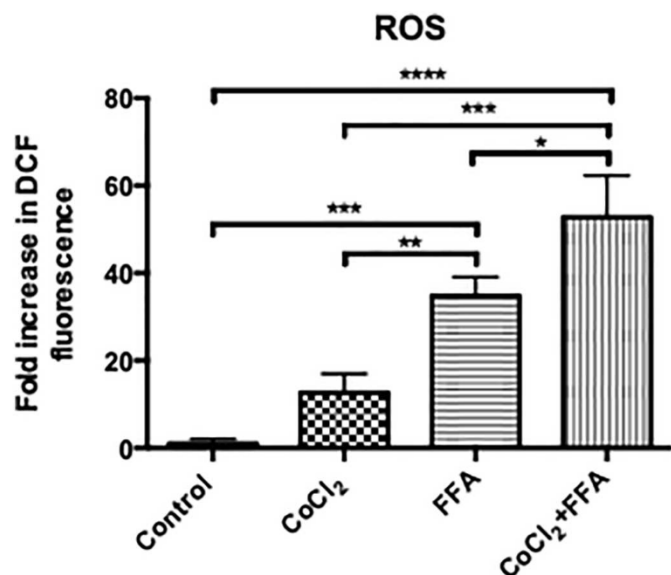re shown as the mean ± SEM ($n \geq 3$) * indicates $P < 0.05$; ** indicates $P < 0.01$; *** indicates $P < 0.005$; **** indicates $P < 0.001$.

Multiple pathogenetic pathways at play may participate in different ways in a given patient, accounting for significant interpatient variability across the disease spectrum and heterogenous clinical phenotypes [5,6]. Comorbidities, particularly type 2 diabetes mellitus, can play a role in modulating the course of NAFLD [7,8]. Clinical observations in patients who suffer from obstructive sleep apnea syndrome (OSAS) have revealed that these patients may also have a higher risk of developing more severe NAFLD associated with significant liver damage [9–11]. OSAS is characterized by intermittent airway obstruction that alters gas exchange leading to periodic hypoxia [12,13], and several studies have demonstrated that hypoxia induces metabolic alterations such as insulin resistance, increased oxidative stress, increased liver

triglyceride accumulation and increased inflammation, hepatocellular damage and fibrogenesis [14–17].

During hypoxia, the transcription factor hypoxia inducible factor 1 alpha (HIF-1α) is stabilized and translocates to the nucleus to activate its target genes by binding of HIF-1α to hypoxia responsive elements (HREs) located in target gene promoters [18]. These target genes modify hepatocyte lipid metabolism as well as energy metabolism, cell survival, inflammation and fibrosis [19–21]. In rodent models of NASH, intermittent hypoxia has been shown to have pro-inflammatory and pro-fibrotic effects, as indicated by increased levels of NF-κB-dependent inflammatory cytokines such as TNF-α, IL-6 and IL-1β, and increased expression of collagen type I in liver [22–24]. Likewise, in vitro studies using hepatocytes and hepatic stellate cells (HSC) have shown that HIF-1α can modulate pro-inflammatory and pro-fibrogenic signaling [20,24–26], which could be key for NASH development and progression.

Involvement of extracellular vesicles (EVs) in the progression of NAFLD has recently been studied using in vitro and in vivo models [27–30]. EVs are classified according to their size and biogenetic origin, e.g., exosomes and microvesicles (28). Exosomes are small particles (50 to 150 nm) that are released after the fusion of multivesicular bodies. Microvesicles are directly released from the cell membrane and have a size of 100 to 1000 nm [31]. In some studies, no distinction was made between microvesicles and exosomes, and the term "EVs" was used for both. EVs play an important role in cellular communication in normal physiological and pathophysiological situations due to their content of proteins, mRNAs and/or lipids [32]. Recent evidence clearly indicates the involvement of EVs in NASH [33,34], but their role in the context of hypoxia and the effects of EVs on nonparenchymal cells, such as HSC, which is the key cell type involved in matrix deposition during liver fibrogenesis, remain to be elucidated.

Therefore, the aim of this study was to test the hypothesis that chemical or intermittent hypoxia leads to hepatocellular damage that determine the release of EVs into the extracellular space that in turn might evoke pro-fibrotic responses on HSC. We used both in vitro and in vivo models to test this hypothesis.
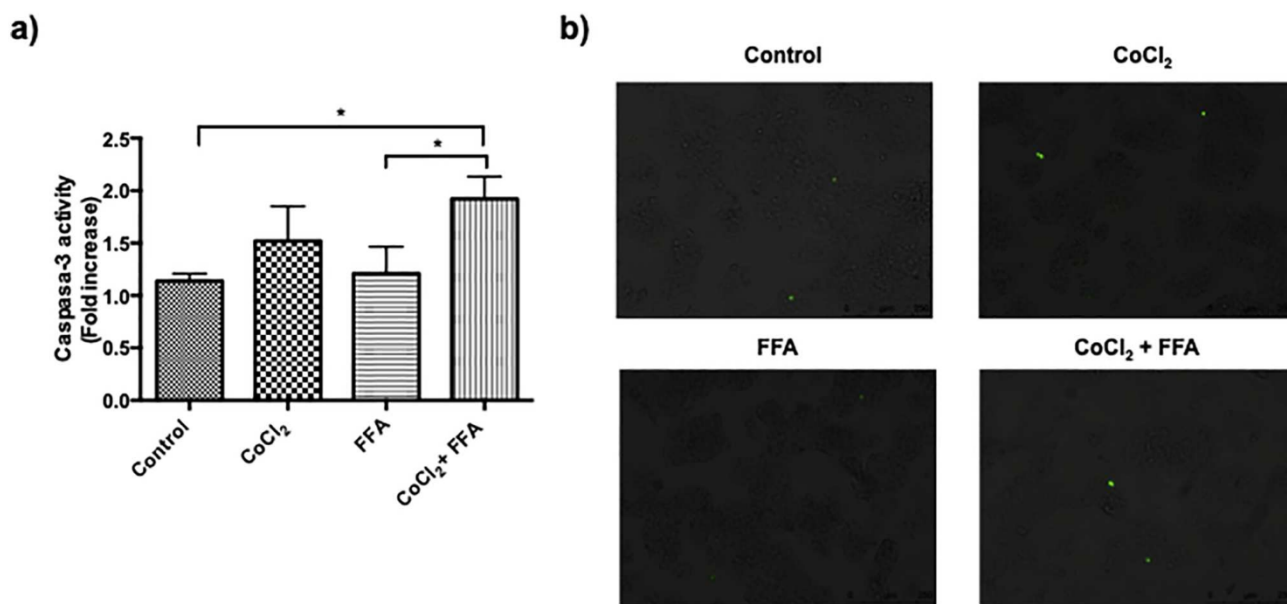

Fig. 4. Chemical hypoxia and steatosis in vitro promote apoptotic cell death but not necrotic cell death. HepG2 cells were incubated for 24 h with oleic acid and [... presen]ce or absence of $CoCl_2$ 200 µmol/l. Caspase-3 activity and necrosis were measured as described in Material and Methods. Data are [... i]ndicates $P < 0.05$.

2. Materials and methods

2.1. Animals

Animal experiments were approved by the institutional animal care and use committee (Comité de ética y bienestar Animal, Escuela de Medicina, Pontificia Universidad Católica de Chile, CEBA 100623003). Male C57BL/6 mice aged 10 weeks at the beginning of the study were divided into four experimental groups ($n = 4$–8) receiving either a choline-deficient amino acid-defined (CDAA) diet (Catalog # 518753, Dyets Inc. Bethlehem, PA) to induce NASH or the choline-supplemented L-amino acid defined (CSAA, Catalog # 518754, Dyets Inc. Bethlehem, PA) diet as a control for 22 weeks as previously described [35,36]. Animals were exposed to IH or normoxia (chambers 41 × 22 × 35 cm, COY lab products™, Grass Lake, MI, USA) during the last 12 weeks of the experimental or control feeding period. The IH regimen consisted of a reduction of the fraction of inspired oxygen (FiO2) from 0.21 to 0.07 over a 30-second period and then reoxygenation to 0.21 FiO2 in the subsequent 30-second period. This regimen was performed for 30 events/h of hypoxic exposure for 8 h/day during the rest cycle, between 9 am and 5 pm. The cycle was repeated 7 days a week for 12 consecutive weeks. After ending the study, the mice were anesthetized (ketamine 60 mg/kg plus xylazine 10 mg/kg intraperitoneally) and then euthanized by exsanguination. Serum and liver tissue samples were collected and processed or stored at $-80\,^\circ$C until analysis.

2.2. Histological studies

Liver specimens from the right lobe of all mouse livers were analyzed in paraformaldehyde-fixed 7-μm tissue sections stained with hematoxylin/eosin or Sirius red. Portal inflammation was graded blindly by an experienced pathologist (J.T.). Specifically, the following score was given: foci of lobular inflammation were scored as 0 (no inflammatory foci), 1 (< 2 foci per 200× field), 2 (2–4 foci per 200× field) and 3 (> 4 foci per 200× field). Sirius red staining to determinate fibrosis was quantified by digital image analysis (Image J, NIH, US) as previously described [35].

2.3. Cell culture and treatment with free fatty acids and chemical hypoxia induction

The human hepatocellular carcinoma cell line HepG2 (ATCC, USA) was cultured in Dulbecco's Modified Eagle's Medium (1X) + GlutaMAX™- I (DMEM, 10569010, Gibco) supplemented with 10% fetal bovine serum (FBS; Gibco) and 1% penicillin-streptomycin (Gibco) at 37 °C and 5% CO_2. All cells were plated in a cell culture plate at least 24 h–36 h before treatment. Upon reaching 80% confluence, the cells were incubated with a mixture of free fatty acids (FFA) consisting of oleic acid (500 μmol/l) and palmitic acid (250 μmol/l) in an aqueous solution of bovine serum albumin (BSA) as previously described [37]. Incubations were carried out with or without cobalt (II) chloride ($CoCl_2$; Sigma-Aldrich, Saint Louis, MO) (200 μmol/l) for 24 h. $CoCl_2$ is the most commonly used hypoxia-mimetic agent [38], which causes
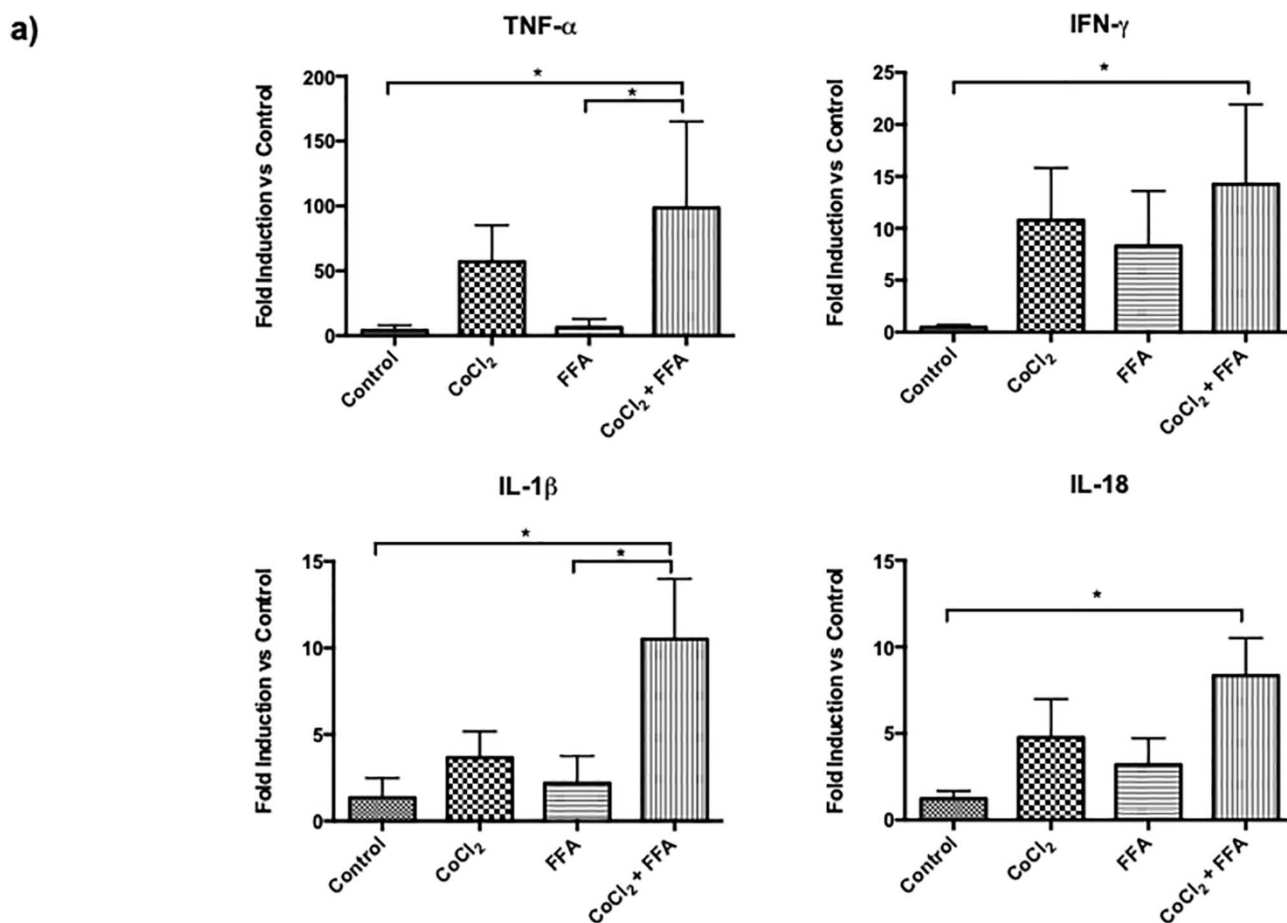
Fig. 5. Chemical hypoxia increases the expression of pro-inflammatory and pro-fibrotic cytokines in steatotic HepG2 cells. HepG2 cells were incubated for 24 h with oleic acid and palmitic acid 2:1 (FFA) in the presence or absence of $CoCl_2$ 200 μmol/l. a) mRNA levels of the pro-inflammatory cytokines TNF-α, IFN-γ, IL-1β, and IL-... ...otic cytokines TGF-β1, CTGF, collagen-I, α-SMA and TIMP-1, measured as described in Material and Methods. Data are shown as ... < 0.05; ** indicates P < 0.01; *** indicates P < 0.005.

b)
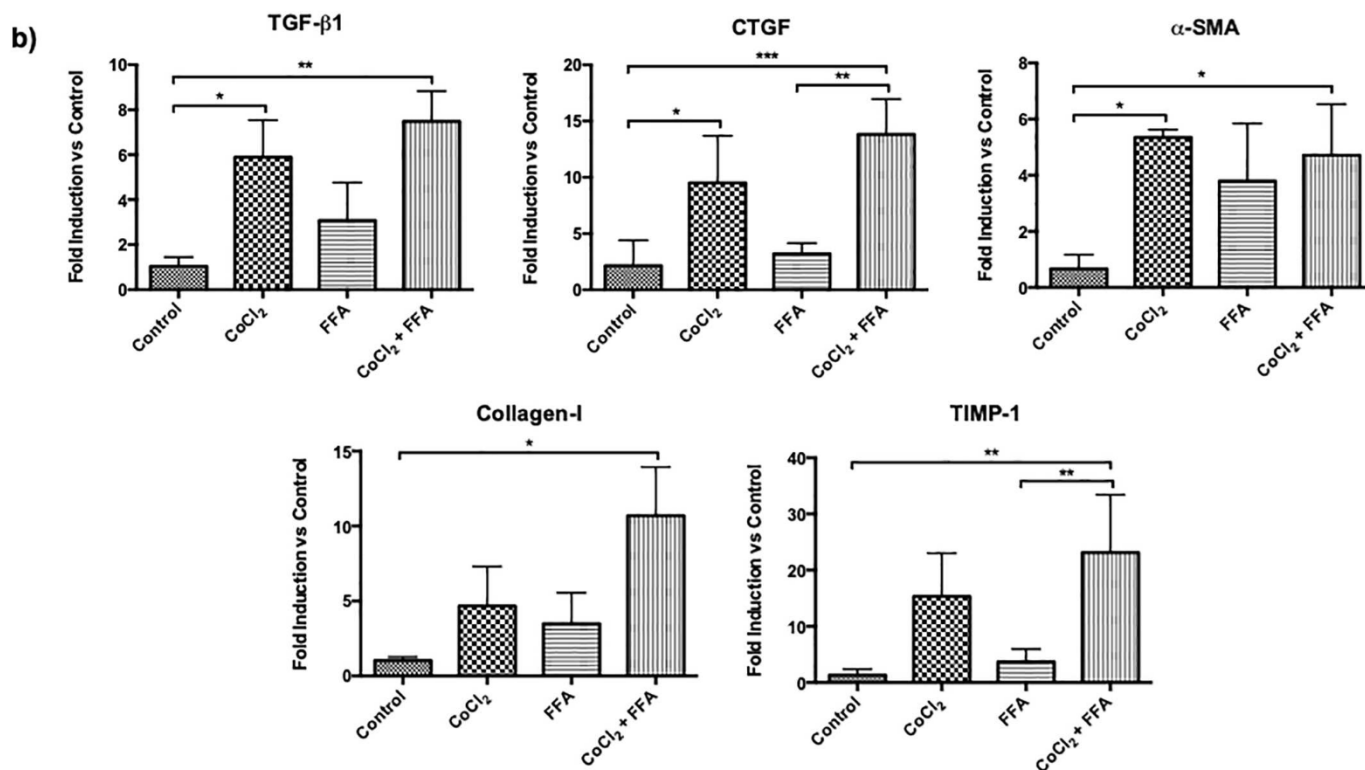
Fig. 5. (*continued*)

chemical hypoxia through stabilization of hypoxia-inducible factor (HIF)-1α [38,39].

2.4. Western blot analyses

Cell lysates were resolved on Mini-PROTEAN® TGX Stain-Free™ Precast Gels (BioRad, Oxford, UK). Semi dry-blotting was performed using a Trans-Blot Turbo Midi Nitrocellulose Membrane with Trans-Blot Turbo System Transfer (BioRad, Oxford, UK). Ponceau S 0.1% w/v (Sigma-Aldrich, Saint Louis, MO) staining was used to confirm the protein transfer. Anti-HIF1α (610,958, Biosciences, San Jose, CA), anti-CASP1 (SC-56036, Santa Cruz, Dallas, TX), anti-CD81 (10630D, Invitrogen, Carlsbad, CA), anti-Bcl-2 (ab32370, Abcam, Cambridge, MA), anti-Type I collagen (1310-01; Southern Biotech, Dallas, TX) and anti-αSMA (A5228, Sigma-Aldrich, Saint Louis, MO) were used in combination with the appropriate peroxidase-conjugated secondary antibodies. Tubulin (T9026, Sigma-Aldrich, Saint Louis, MO) or actin (A5228, Sigma-Aldrich, Saint Louis, MO) was used as a loading control. The blots were analyzed with a ChemiDoc XRS system (Bio-Rad, Oxford, UK). Protein band intensities were quantified by ImageLab software (BioRad, Oxford, UK).

2.5. Nile red staining

Intracellular lipid droplets in the HepG2 cells were detected with Nile Red fluorescent probe (N1142, Thermo Fisher, Wilmington, DE). HepG2 cells were grown in 96-well plates and treated with FFA and/or CoCl_2. After treatment, the cells were washed twice with PBS and stained with Nile Red solution for 10 min in the dark. The cells were then washed twice with PBS and stained with Hoechst dye (33342, Thermo Fisher, Wilmington, DE). The fluorescence intensity of each well was analyzed with an excitation/emission wavelength at 488 nm/ [...]er. The fluorescence images were re-[...]ce microscope.

2.6. Determination of reactive oxygen species

The intracellular generation of reactive oxygen species (ROS) in HepG2 cells was monitored with a DCFH-DA fluorescent probe. HepG2 cells were grown in 96-well plates and treated with FFA and/or CoCl_2. Cells were washed twice with PBS and incubated with the cell permeable reagent 2′,7′–dichlorofluorescin diacetate (DCFDA; Abcam, Cambridge, MA) for 45 min. Cells were then washed twice with PBS, and the fluorescence intensity of each well was analyzed with an excitation/emission wavelength at 495 nm/529 nm using a microplate reader.

2.7. Apoptosis measurement

The caspase-3 fluorometric assay was used to determine apoptosis induced by FFA and/or CoCl_2 in HepG2 cells. After treatment, HepG2 were scraped, and cell lysates were obtained by three cycles of freezing (−80 °C) and thawing (37 °C) followed by centrifugation for 5 min at 13,000g. Caspase-3 enzyme activity was assayed as described previously [40]. The arbitrary units of fluorescence (AUF) were quantified in a spectrofluorometer at an excitation wavelength of 380 nm and emission wavelength of 430 nm.

2.8. Assessment of cell death associated with disrupted cellular membrane integrity

SYTOX® Green nucleic acid stain (S7020 Invitrogen, Carlsbad, CA) was used to determine cell death induced by FFA and/or CoCl_2 in HepG2 [41]. Cells were cultured in 12-well plates. After treatment, diluted Sytox Green solution (1:40.000/PBS) was added to the cells for at least 15 min at 37 °C, 5% CO_2. Necrotic cells have ruptured plasma membranes, allowing the noncell permeable Sytox Green to enter the cells and bind to nucleic acids. Necrosis was determined using a Leica fluorescence microscope at a wavelength of 488 nm.
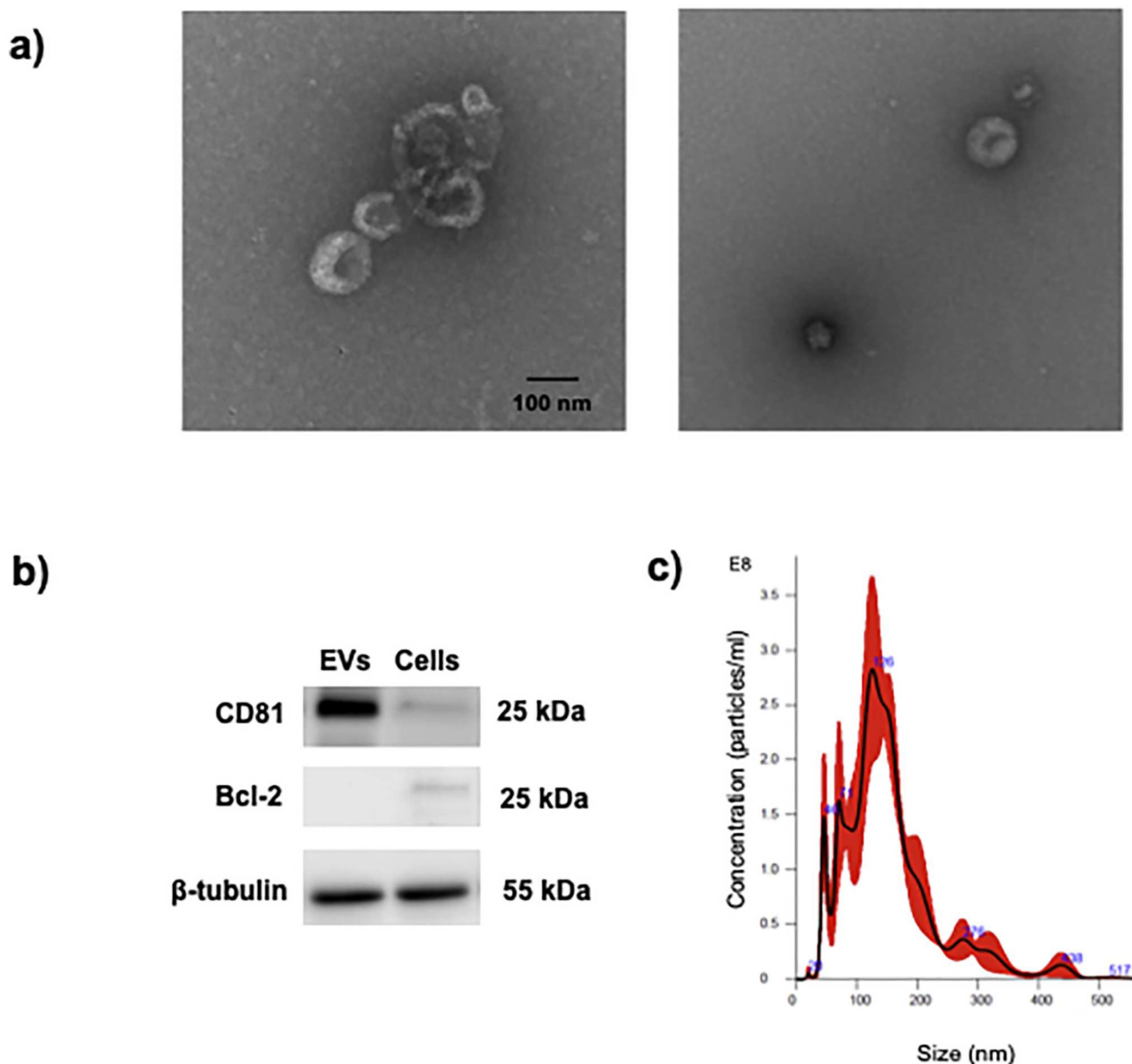
Fig. 6. Characterization of HepG2-derived extracellular vesicles (EVs). EVs were characterized in conditioned medium from control HepG2 cells by a) transmission electron microscopy, b) detection of the EV-positive marker CD81 and EV-negative mitochondrial marker Bcl-2 by Western blotting, and c) size distribution by NTA as described in Material and Methods.

2.9. RNA isolation and quantitative real-time reverse transcription polymerase chain reaction (qRT-PCR)

HepG2 cells were harvested on ice and washed twice with ice-cold PBS. Total RNA was isolated with TRI-reagent (Sigma-Aldrich, Saint Louis, MO) according to the manufacturer's instructions. Reverse transcription (RT) was performed using 2.5 μg of total RNA, 1X RT buffer (500 mmol/l Tris-HCl [pH 8.3]; 500 mmol/l KCl; 30 mmol/l MgCl$_2$; 50 mmol/l DTT), 1 mmol/l deoxynucleotides triphosphate (dNTPs, Sigma-Aldrich, Saint Louis, MO), 10 ng/μl random nanomers (Sigma-Aldrich, Saint Louis, MO), 0.6 U/μl RNaseOUT™ (Invitrogen, Carlsbad, CA) and 4 U/μl M-MLV reverse transcriptase (Invitrogen, Carlsbad, CA) in a final volume of 50 μl. The cDNA synthesis program was 25 °C/10 min, 37 °C/60 min and 95 °C/5 min. Complementary DNA (cDNA) was diluted 20× in nuclease-free water. Real-Time qPCR was carried out in a StepOnePlus™ (96-well) PCR System (Applied Biosystems, using TaqMan probes. The sequences

of the probes and primer sets are described in Supplementary Material. For qPCR, 2× reaction buffer (dNTPs, HotGoldStar DNA polymerase, 5 mmol/l MgCl$_2$) (Eurogentec, Belgium, Seraing), 5 μmol/l fluorogenic probe and 50 μmol/l of sense and antisense primers (Invitrogen) were used. mRNA levels were normalized to the 18S housekeeping gene and further normalized to the mean expression level of the control group.

2.10. Extracellular vesicle isolation

For EV collection, HepG2 cells were grown in culture dishes of 100 mm to obtain 70 ml of serum-free conditioned medium (devoid of CoCl2 or FFA) after different treatments for an additional 24 h. EVs were isolated from the conditioned medium by differential ultra-centrifugation (UCF Thermo-Sorvall 80wx+) according to a modified previous protocol [42]. A total of 70 ml medium per treatment was depleted of cells and cell debris by consecutive, low-speed centrifugations (2000 ×g for 30 min and 12,000 ×g for 45 min). The resulting

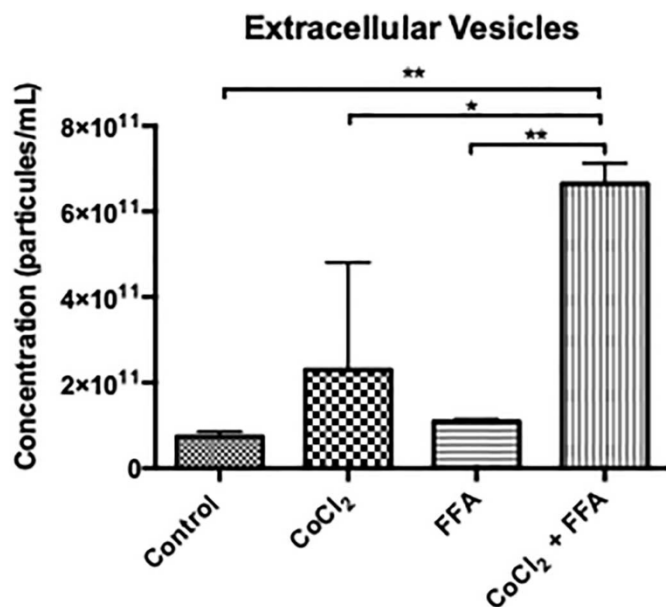**Fig. 7.** Increased release of extracellular vesicles (EVs) from steatotic HepG2 cells undergoing chemical into conditioned medium. EV quantification in conditioned medium from HepG2 after different treatments performed by NTA as described in Material and Methods. Data are shown as the mean ± SEM (n ≥ 3) * indicates $P < 0.05$; ** indicates $P < 0.01$.

supernatants were carefully collected and centrifuged for 70 min at 120,000 $\times g$ at 4 °C. Pellets from this centrifugation step were washed in PBS, pooled and centrifuged again for 60 min at 100,000 $\times g$ at 4 °C. For EV collection from animals, serum samples were reconstituted in a total volume of 4.4 ml and centrifuged at 2000 $\times g$ for 30 min and 10,000 $\times g$ for 30 min. The resulting supernatants were carefully collected and centrifuged for 70 min at 120,000 $\times g$ at 4 °C. Pellets from this centrifugation step were washed in PBS, pooled and centrifuged again for 60 min at 100,000 $\times g$ at 4 °C. The obtained pellets from HepG2 cells or serum were resuspended in lysis buffer or PBS solution depending on subsequent experiments and stored in aliquots at −80 °C. Protein concentration in the EV pellet was measured using the BCA protein assay kit (Pierce, Rockford, IL).

2.11. Nanoparticle tracking analysis

Concentration and size distribution of isolated EVs were assessed by nanoparticle tracking analysis (NTA) using NanoSight NS300 instrumentation (Marvel, Egham, UK). EV samples were diluted with PBS to a concentration of 10^8 to 10^9 particles/ml in a total volume of 1 ml. Each sample was continuously run through a flow-cell top-plate set up at 18 °C using a syringe pump. At least three videos of 20 s documenting the Brownian motion of nanoparticles were recorded, and at least 1000 completed tracks were analyzed using NanoSight software (NTA v3.2).

2.12. Transmission electron microscopy

Isolated EVs were fixed in 2% paraformaldehyde in 0.1 M phosphate buffer overnight at 4 °C. The samples were then placed on a Formvar/Carbon 300 Mesh (FCF300-CU, EMS) grid and air dried for 10 min. The grids were first contrasted with uranyl-oxalate solution and then contrasted and embedded in a mixture of 4% uranyl acetate. The grids were air dried and visualized using a Philips Tecnai 12 (Biotwin, Eindhoven, The Netherlands) electron microscope at 80 kV. The images were cap- ... Imaging Solutions software (Windows

2.13. Treatment of LX-2 cells with extracellular vesicles

To investigate the crosstalk between EVs from HepG2 and LX-2 human HSC, a typical cell line to study hepatic fibrogenesis [43], LX-2 cells were treated with isolated EVs. LX-2 cells were cultured in DMEM supplemented with 10% FBS and 1% penicillin-streptomycin at 37 °C and 5% CO_2. All cells were plated in a cell culture plate at least 24–36 h before treatment. Upon reaching 80% confluence, the cells were incubated with FBS-free medium and exposed to 15 μg of EVs that were isolated from HepG2 cells that had been treated with $CoCl_2$, FFA and $CoCl_2$ + FFA for 24 h. After 24 h of EV treatment, LX-2 cells were harvested for further quantitative PCR, Western blot and immuno-fluorescence analyses.

2.14. Immunofluorescence microscopy

LX-2 cells were grown on glass cover slips placed in 12-well plates. After treatment, the culture media were removed and cover slips carefully washed twice with PBS. Cells were then fixed using a 4% paraformaldehyde solution in PBS for 10 min at room temperature and washed twice with PBS. Permeabilization was performed by incubation of the samples for 10 min in 0.1% Triton X-100 (Sigma-Aldrich, Saint Louis, MO). The cells were washed twice with PBS and incubated with 2% BSA (Sigma-Aldrich, Saint Louis, MO) in PBS/0.1% Tween 20 (Sigma-Aldrich, Saint Louis, MO) solution for 30 min to block non-specific binding sites. Goat anti-Type I collagen (1310-01; Southern Biotech, Birmingham, AL) was used at a dilution of 1:200 in 2% BSA/PBS in a humidified chamber for 1 h at room temperature. Samples were subsequently washed twice with 2% BSA/PBS. Finally, the cells were incubated with rabbit anti-goat Alexa Fluor® 568 at a dilution of 1:500 in 2% BSA/PBS for 30 min at room temperature in the dark. Slides were mounted with ProLong antifade with DAPI (Molecular Probes, Invitrogen™, Carlsbad, CA, USA), and images were evaluated using fluorescence microscopy and analyzed with Leica ALS AF software (Leica, (Leica Microsystems GmbH, Wetzlar).

2.15. Statistical analyses

Analyses were performed using GraphPad software (version 5.03, GraphPad Software Inc., CA, USA). All results are presented as the mean of at least 3 independent experiments ± SEM or as absolute numbers or percentages for categorical variables. The statistical significance of differences between the means of the experimental groups was evaluated using one-way analysis of variance (ANOVA) with a *post hoc* Bonferroni multiple-comparison test; $P < 0.05$ was considered as statistically significant.

3. Results

3.1. Chemical hypoxia increases lipid droplet content in fat-laden hepatic cells

To investigate whether hypoxia exacerbates lipid accumulation in an *in vitro* model of experimental NASH, we treated HepG2 cells with $CoCl_2$, a hypoxia mimetic agent that promotes the accumulation of HIF-1α [38]. HepG2 cells treated with $CoCl_2$ showed a significant increase in HIF-1α, independent of treatment with FFA (Fig. 1). To induce steatosis, HepG2 cells were treated with a mixture of oleic acid and palmitic acid (FFA) as described previously [44]. Hepatocytes showed an increase in the formation of lipid droplets (Fig. 2a). Interestingly, a significant increase in the content of lipid droplets was observed in the steatotic hepatocytes treated with the chemical inducer of hypoxia (Fig. 2b), indicating that chemical hypoxia increases steatosis in this model.
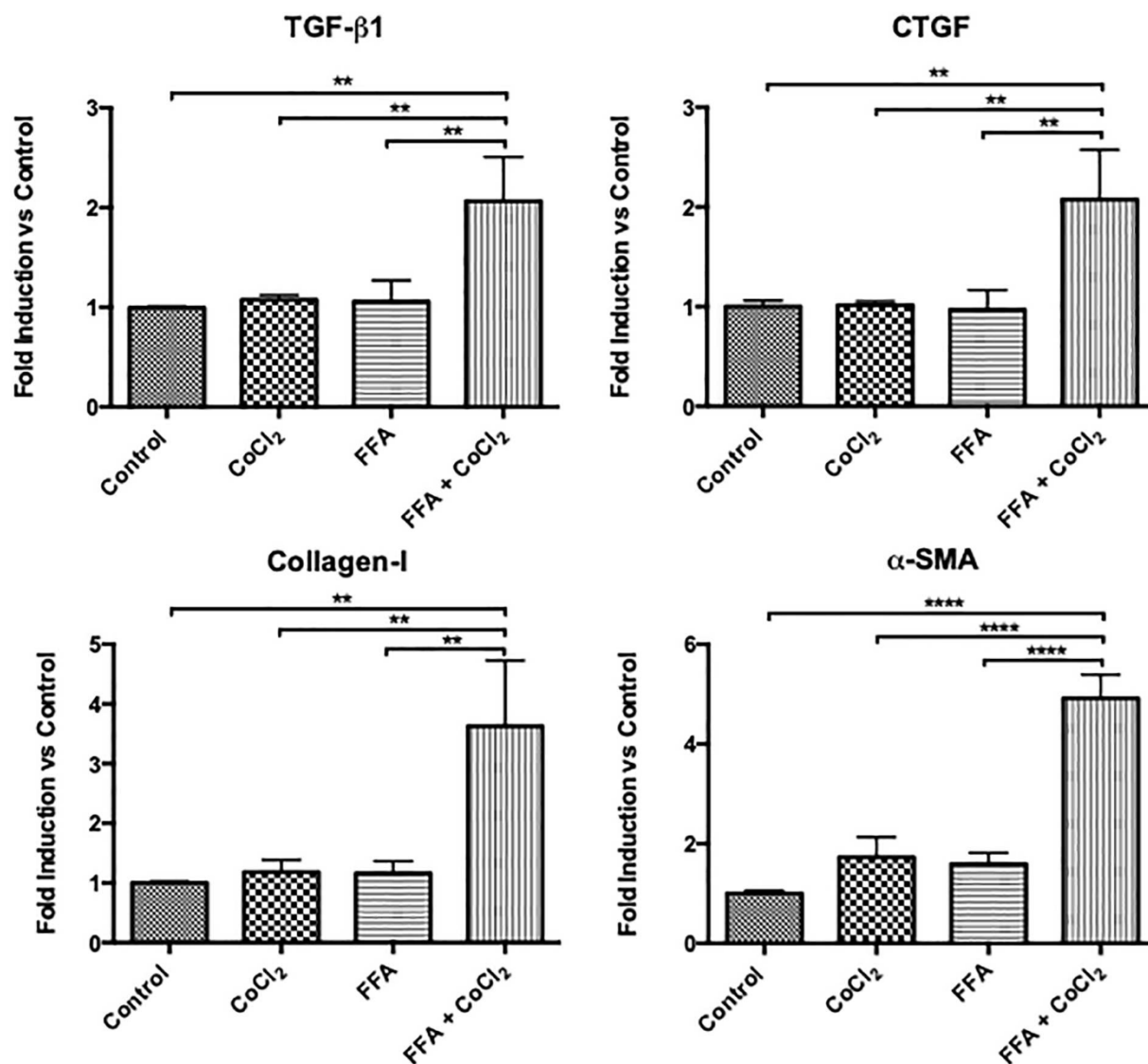
Fig. 8. HepG2-derived extracellular vesicles (EVs) increase the expression of pro-fibrotic cytokines in LX-2 cells. LX-2 cells were exposed to 15 μg of EVs that were isolated from HepG2 cells that had been treated with CoCl₂, FFA and CoCl₂ + FFA for 24 h. mRNA levels of TGF-β1, CTGF, collagen-I and α-SMA were measured as described in Material and Methods. Data are shown as the mean ± SEM (n ≥ 3) ** indicates $P < 0.01$; **** indicates $P < 0.001$.

3.2. Chemical hypoxia increases oxidative stress and apoptotic cell death in fat-laden hepatic cells

To evaluate whether the induction of hypoxia exacerbates damage by lipotoxicity, we evaluated the generation of reactive oxygen species (ROS) and the extent of cell death. The increase in ROS was evaluated using the fluorogenic dye DCF. The results indicated a significant increase in ROS in each of the treatments compared with the control (Fig. 3). Furthermore, chemical hypoxia exacerbated the increase in ROS in steatotic HepG2 cells compared with the hypoxic and FFA conditions separately.

Apoptotic cell death was evaluated by measuring the activity of caspase-3. The results demonstrated that chemical hypoxia in steatotic HepG2 cells induced apoptotic lipotoxicity compared with the control cells. (Fig. 4a). Chemical hypoxia or steatosis alone did not induce apoptotic cell death. Lipotoxicity was also evaluated using the Sytox Green assay to detect cell death associated with disrupted cellular membrane integrity. The different treatments in HepG2 cells did not induce necrotic cell death (Fig. 4b).

3.3. Chemical hypoxia induces the expression of pro-inflammatory and pro-fibrotic cytokines

To evaluate whether hypoxia promotes a pro-inflammatory and pro-fibrotic phenotype in fat-laden HepG2 cells, we measured the mRNA levels of different cytokines. A significant increase in mRNA levels of pro-inflammatory (Fig. 5a) and pro-fibrotic (Fig. 5b) cytokines was observed. Expression of some genes was also increased in cells treated with CoCl₂ only (Fig. 5b).

3.4. Increased number of EVs in conditioned medium from steatotic cells undergoing chemical hypoxia

To better characterize the involvement of hepatocytes in the promotion of the pro-fibrotic phenotype and possible crosstalk with HSC, we assessed EVs from conditioned medium of HepG2 cells (HepG2-EV) following different treatments. After isolation of EVs from conditioned medium, we characterized EVs according to previous guidelines [45] by their typical structure visualized by TEM (Fig. 6a) and detection of the EV-positive marker CD81 and EV-negative marker Bcl-2 (mitochondrial marker) by Western blotting (Fig. 6b). We also determined the size

(approximately 100–150 nm) and concentration of HepG2-EV (Fig. 6c) by NTA. Notably, fat-laden-hepatocytes in the presence of $CoCl_2$ showed a significant increase in the concentration of HepG2-EV compared with all other conditions (Fig. 7). These results suggest that steatotic and hypoxic conditions in HepG2 cells can modulate the release of EVs.

3.5. EVs from steatotic HepG2 cells undergoing chemical hypoxia promote a pro-fibrotic phenotype in HSC

To evaluate whether HepG2-EVs have a direct effect on HSC, we used the human stellate cell line LX-2. LX-2 cells were stimulated with 15 μg/ml of HepG2-EV from each treatment, and the mRNA and protein levels of some pro-fibrotic cytokines were evaluated. As shown in Fig. 8, EVs from steatotic HepG2 cells undergoing chemical hypoxia significantly increase the expression levels of the TGF-β-1, CTGF, collagen-I and α-SMA genes in LX-2 cells. These results also suggest an additive effect of FFA and $CoCl_2$ promoting a pro-fibrotic phenotype in LX-2 cells. Interestingly, a similar result was observed in a confirmatory experiment assessing protein levels of collagen-I (Fig. 9a–c) and α-SMA (Fig. 9b) in LX-2 cells treated with EVs obtained from fat-laden HepG2 cells undergoing chemical hypoxia.

3.6. Intermittent hypoxia promotes a pro-inflammatory and pro-fibrotic phenotype that correlates with increased release of EVs in an in vivo model of NASH

To validate the previous results in an *in vivo* model, CDAA diet feeding for 22-weeks was used to induce NASH, and an intermittent

hypoxia regimen was applied for the final 12 weeks. As expected, CDAA diet-fed mice showed significantly increased portal inflammation (Fig. 10a) and liver fibrosis (Fig. 10b), as shown by conventional hematoxylin/eosin and Sirius Red staining, respectively. Interestingly, portal inflammation and collagen deposition in IH-treated mice with NASH were even further increased compared with the normoxic CDAA diet-group, indicating a pro-inflammatory and pro-fibrotic action of hypoxia. In addition, IH significantly increased hepatic mRNA levels of several markers of inflammation (Fig. 10c) and fibrogenesis (Fig. 10d) induced by the CDAA diet, including HIF-1α, IL-6, TNF-α, IFN-γ, IL-1β, IL-18, TGF-β1, CTGF, collagen-I, α-SMA, TIMP-1 and MCP-1, compared to the control group. Only IL-6, IFN-γ, IL-18 and α-SMA mRNA levels were significantly increased in mice with NASH exposed to IH compared with normoxic mice with NASH. Finally, EVs were isolated from mouse serum to determine the concentration of EVs in each experimental group. As shown in Fig. 10e, CDAA diet-fed mice exhibited a significant increase in EVs when exposed to IH compared with control or CDAA diet-fed mice under normoxic conditions. These results suggest a strong correlation between the induction of intermittent hypoxia with the increase in EVs and the promotion of a more pro-inflammatory and pro-fibrotic phenotype in an *in vivo* model of NASH.

4. Discussion

In recent years, the mechanisms underlying the progression of NAFLD/NASH have been thoroughly studied. The early stages of NAFLD are characterized by fat accumulation in the liver resulting in steatosis that can progress to hepatocellular damage and inflammation in a condition termed NASH [3–6]. Moreover, some patients develop
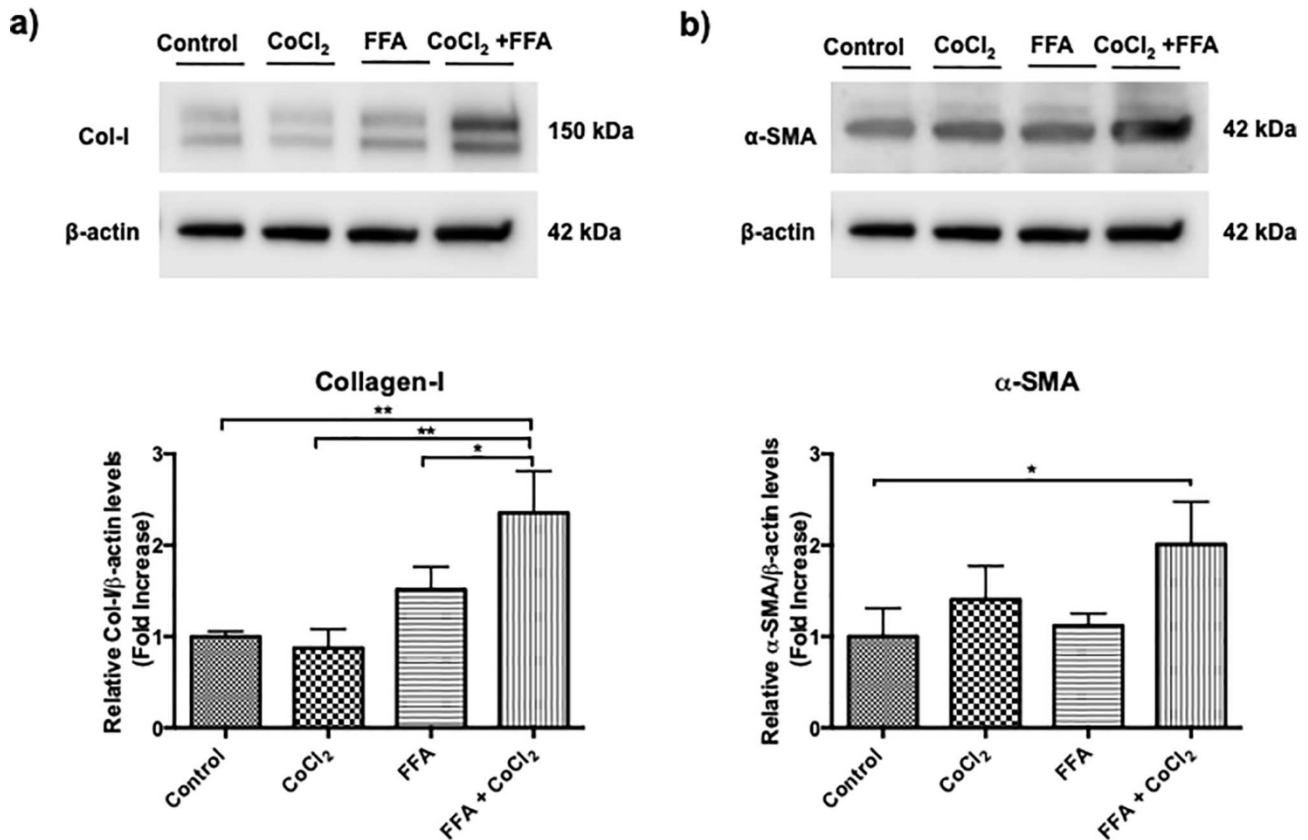
Fig. 9. Extracellular vesicles (EVs) derived from steatotic HepG2 cells undergoing chemical hypoxia increase the expression of pro-fibrotic proteins in HSC. LX-2 cells were exposed to 15 μg of EVs that were isolated from HepG2 cells that had been treated with $CoCl_2$, FFA and $CoCl_2$ + FFA for 24 h. Protein levels of a) collagen-I and b) alpha-smooth muscle actin (α-SMA) were determined by Western blotting as described in Materials and Methods. β-actin was used as loading control. c) [...] [wa]s determined by immunofluorescence as described in Materials and Methods. Data are shown as the mean ± SEM (n ≥ 3) * [...] [P <] 0.01; *** indicates P < 0.005.

c)
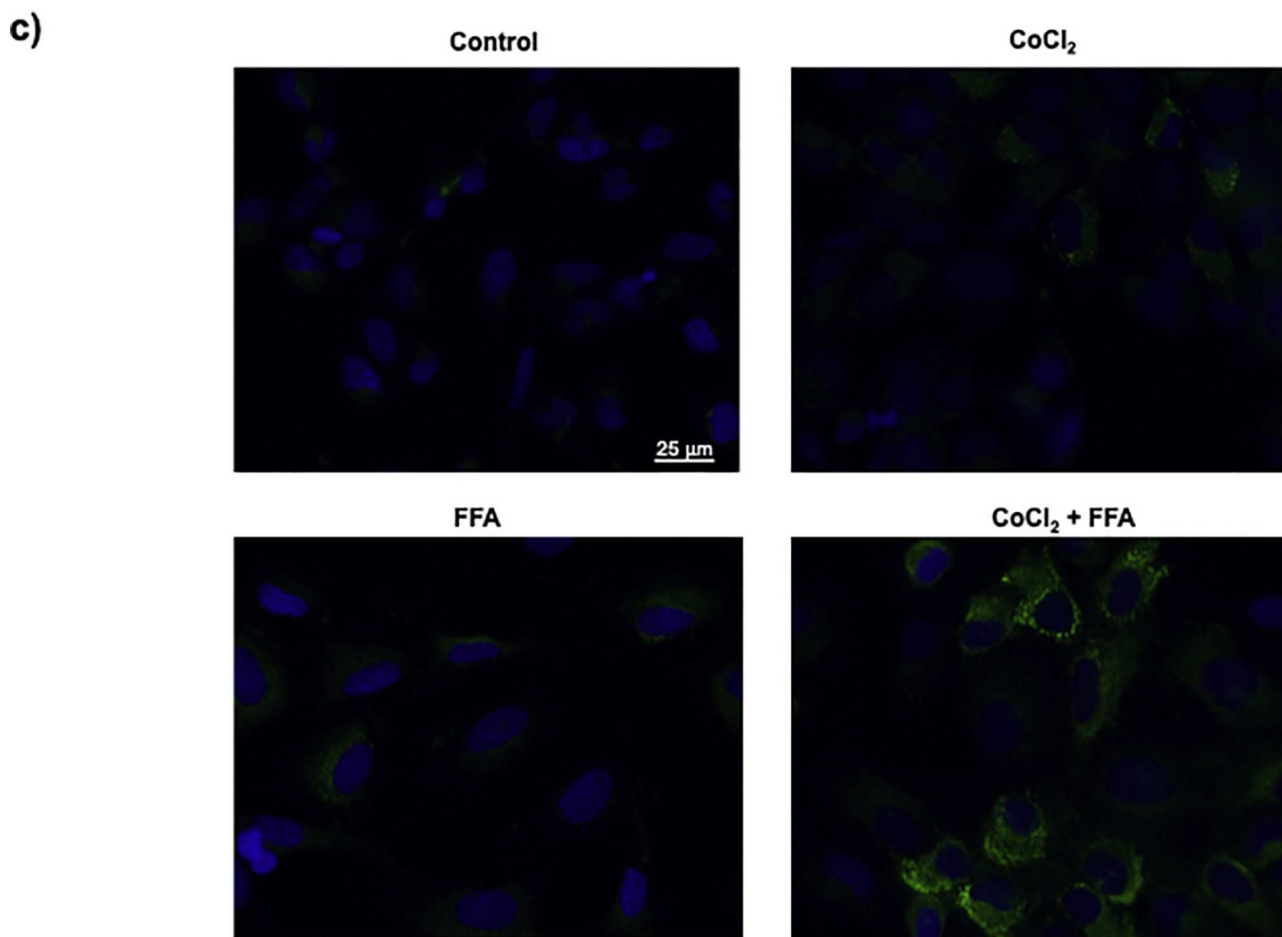
Fig. 9. (*continued*)

liver fibrosis, which is associated with an increase in mortality and the risk of HCC development [46]. Interestingly, clinical studies have indicated that OSAS is a new predictive factor of hepatic fibrosis in patients with NAFLD [10,47,48]. Recent research has provided evidence regarding the role of hypoxia, a hallmark of OSAS, in the development of liver injury and hepatic fibrosis in animal models of NAFLD [20,22,49]. However, major gaps remain in our understanding of the progression of NASH to fibrosis, *e.g.*, the cellular mechanism underlying crosstalk between hepatocytes and HSC, the key nonparenchymal cell responsible for liver scar formation [50,51]. In this study, we demonstrate that experimental hypoxia, induced by a HIF-1α chemical stabilizer in fat-laden liver cells, promotes hepatocellular damage, enhances pro-inflammatory and pro-fibrogenic gene expression and increases the release of EVs. Furthermore, EVs from steatotic HepG2 cells undergoing Cocl2 chemically induced hypoxia promote increases in the mRNA and protein expression of important fibrosis markers in HSC.

In the present study, our *in vitro* model of steatosis was key to the analysis of hypoxia induced by the hypoxia mimetic CoCl2, a HIF-1 α stabilizer. We used the human hepatocyte cell line HepG2, in which induction of chemical hypoxia was evaluated through the quantification of HIF-1α levels, which increased due to the intracellular stabilization, as described in other *in vitro* studies [52,53]. Of note, treatment with palmitic acid (PA) and oleic acid (OA) (1:2) increased the content of lipid droplets in hepatocytes in the absence of lipotoxicity. Previous studies have shown that OA promotes steatosis in hepatocytes, both in primary hepatocyte cultures and in hepatoma cell lines, while PA induces a cytotoxic response [54,55]. Our results are in line with a previous report using a combination of both fatty acids at a higher OA anti-apoptotic effect and triglyceride

accumulation [54]. Interestingly, chemical hypoxia increased the content of lipid droplets compared with HepG2 cells without chemical hypoxia, as determined by quantification of Nile Red fluorescence. These results are in line with an *in vivo* study indicating that hypoxia, *via* HIF-1α, promotes an increase in lipid biosynthesis [56]. Hepatocyte cell death by apoptosis was measured using caspase-3, and as expected, treatment with FFA alone did not induce cell death. However, HepG2 cells exposed to the combination of treatment with CoCl2 and FFA exhibited an increase in caspase-3 activity that correlated with an increase in oxidative stress compared with the control group. Unexpectedly, HepG2 cells treated with FFAs also showed an increase in ROS compared with those treated with CoCl2 and the control group. A recent study demonstrated that OA prevents ROS production in HepG2 cells treated with PA [57]. Likewise, another study showed that FFA treatment of HepG2 cells induced TNF-α generation, which is an important mediator in hepatic steatohepatitis and liver injury [58]. Additional studies to further delineate the underlying mechanism, *e.g.*, measurement of mitochondrial ROS production, remain to be performed. We also analyzed hepatocyte cell death associated with disrupted cellular membrane integrity (necrosis) using SytoxGreen®. None of the treatments we applied induced a significant increase in necrosis. The divergent results of apoptosis and necrosis can be explained by the potential of different stimuli to induce different modes of cell death in different cell types [59]. Taken together, our findings indicate that chemical hypoxia promotes lipotoxicity, as determined by the increase in hepatocellular apoptosis and oxidative stress.

To evaluate the possible damaging effects of chemical hypoxia in fat-laden hepatocytes, we measured the gene expression of pro-inflammatory and pro-fibrotic cytokines. As expected, and in accordance
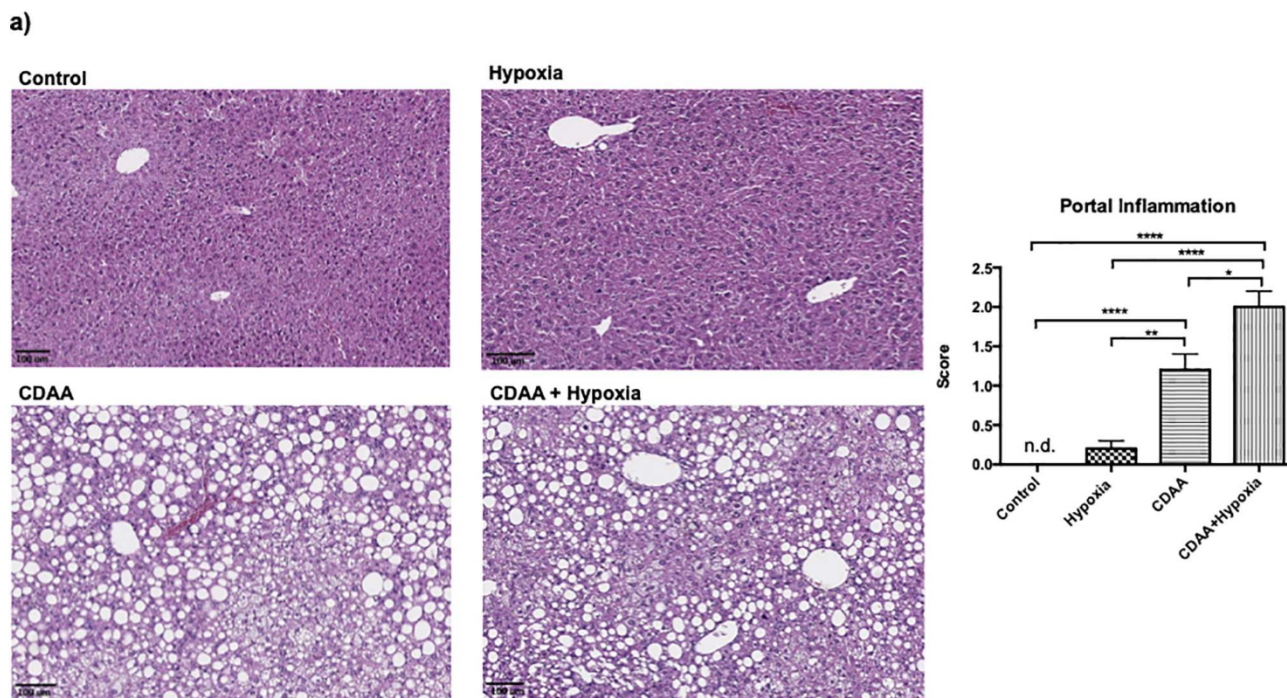
a)

Fig. 10. Intermittent hypoxia promotes a pro-fibrotic phenotype in mice with NASH and correlates with increased levels of extracellular vesicles (EVs) *in vivo*. Mice were placed on a choline-supplemented L-amino acid defined (CSAA) diet as a control or a defined diet with choline deficiency amino acids (CDAA) for 22 weeks to induce liver injury. Intermittent hypoxia (IH) or normoxia was applied for the final 12 weeks of the diet as described in Materials and Methods. Representative histology of liver tissue: a) hematoxylin/eosin staining to evaluate portal inflammation and b) Sirius Red staining to evaluate fibrosis were scored in a double blinded manner by a pathologist; c) mRNA levels of pro-inflammatory cytokines and d) mRNA levels of pro-fibrotic cytokines were determined by RT-qPCR as described in Materials and Methods; e) quantification of EVs from serum samples was determined by NTA as described in Materials and Methods. Data are shown as the mean ± SEM (n ≥ 3) * indicates P < 0.05; ** indicates P < 0.01; *** indicates P < 0.005; **** indicates P < 0.001.

b)
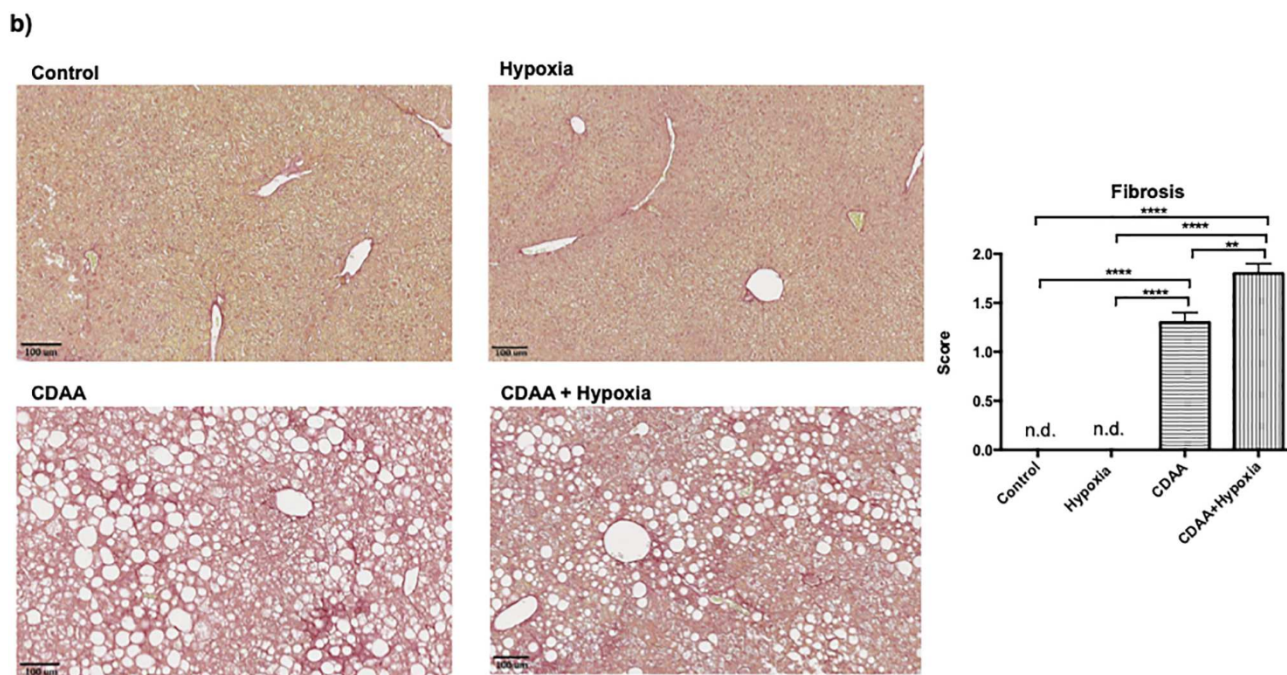
Fig. 10. (*continued*)

with our previous results, the condition of hypoxia in steatotic hepatocytes increased the expression of TNF-α, IFN-γ, IL-1β, IL-18, TGF-β1, CTGF, collagen-I, α-SMA and TIMP-1. Interestingly, some pro-fibrotic genes, such as TGF-β1, CTGF and α-SMA, were increased in HepG2 cells [...] ce of FFAs. Previous data have de- [...] IF-1α in hepatocytes actives TGF-β

signaling and promotes fibrogenesis in liver [24,25]. To evaluate the role of EVs in this model, we assessed the amount of EVs released in the culture medium and observed an increase after treatment of HepG2 cells with CoCl₂ and FFA compared with all other groups. EVs, comprising exosomes and microparticles, are small structures that are surrounded by membrane and released from cells into the extracellular

11
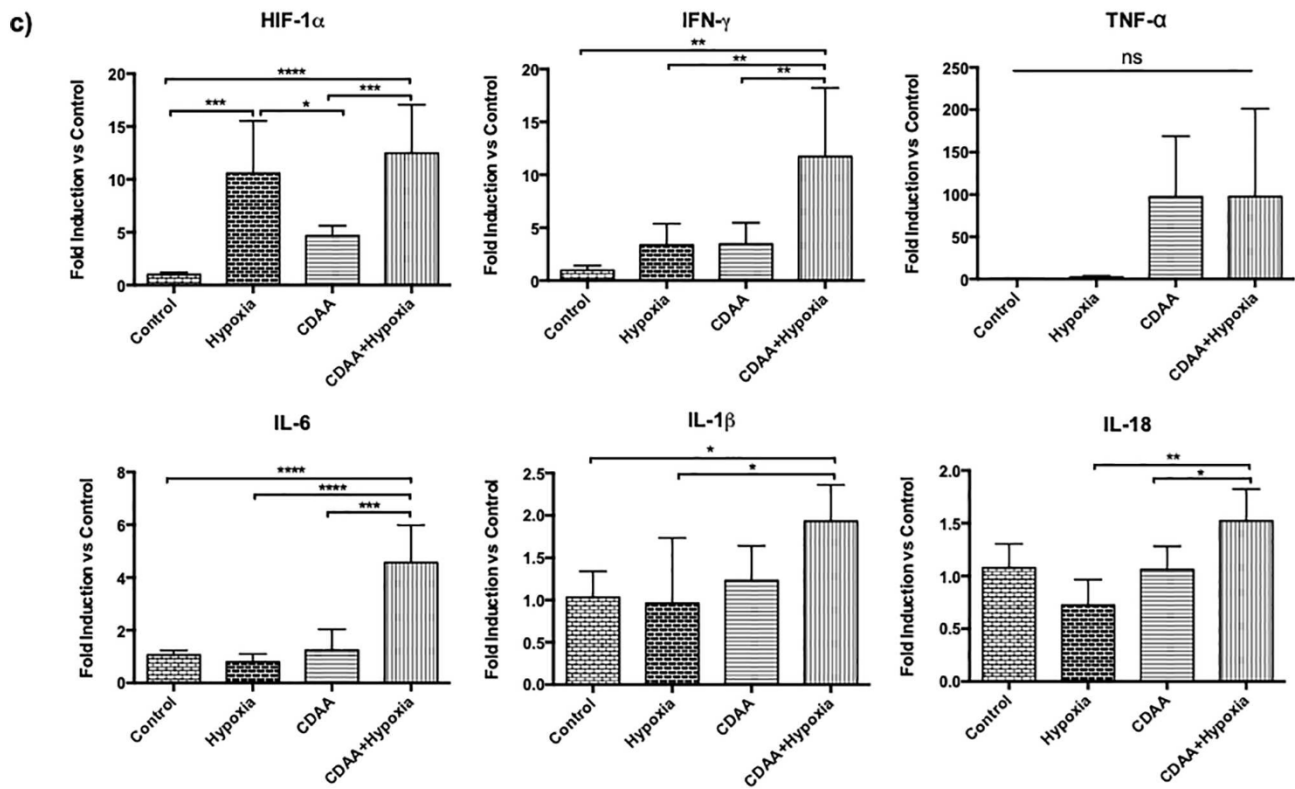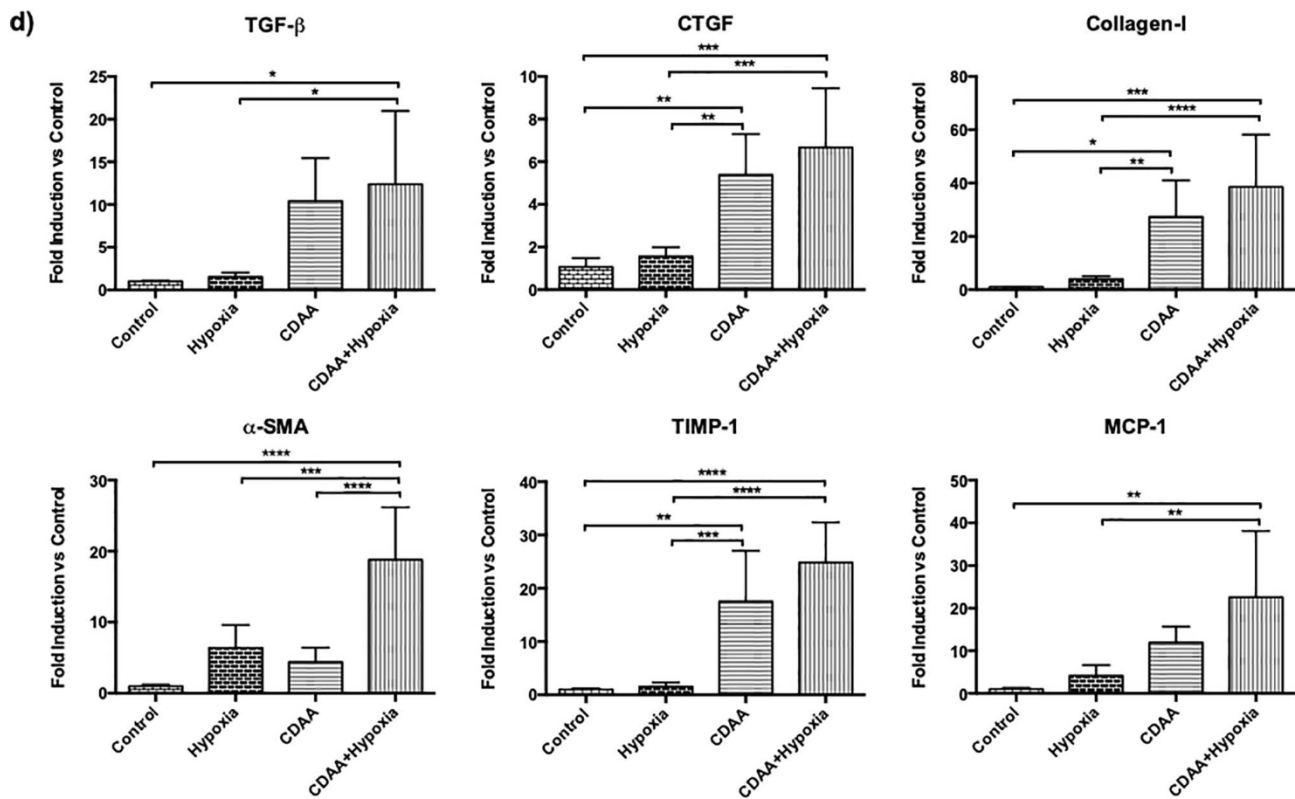
Fig. 10. (*continued*)

Fig. 10. (*continued*)

environment. They serve a pathophysiological role in various diseases, including NASH and other chronic liver diseases [33,34,60]. We characterized the isolated EVs from HepG2 cells using positive and negative ~~~~ determined the EV size by NTA.

Finally, isolated EVs from control hepatocytes were directly visualized using TEM.

Previous studies have demonstrated that during hepatocellular damage, hepatocytes release EVs that modulate pro-inflammatory and

e)
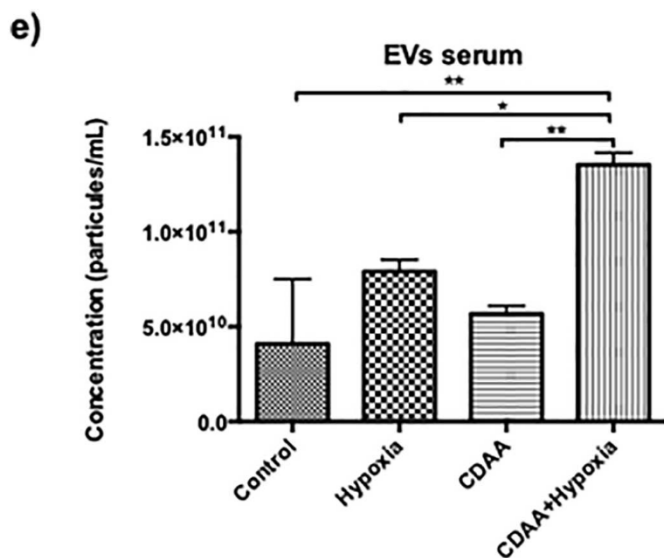
Fig. 10. (*continued*)

pro-fibrotic signaling in nonparenchymal liver cells [61–65]. To confirm whether EVs from our model of hypoxic and steatotic hepatocytes could promote a pro-fibrotic phenotype in nonparenchymal liver cells, we used the human stellate cell line LX-2. EVs derived from $CoCl_2$-treated fat-laden hepatocytes showed increased gene expression of pro-fibrotic cytokines such as TGF-β1, CTGF, collagen-I and α-SMA in LX-2 cells compared with all the other groups. In addition, protein expression of collagen-I and α-SMA was analyzed in LX-2 cells treated with EVs from HepG2 cells. Both pro-fibrotic proteins increased when LX-2 cells were treated with EVs derived from $CoCl_2$-treated steatotic hepatocytes. This interesting result suggests that the EV-cargo in our model is an important topic for future analysis. Recent studies supporting our findings show that palmitic acid increases EVs from hepatocytes and alters their miRNA cargo to induce pro-fibrogenic signals in HSCs [62]. Another study, providing similar results, indicated that EVs from lipotoxic hepatocytes activate HSCs *via* miRNA-128-3p [28].

The exact relationship(s) between intermittent hypoxia, a hallmark of OSAS, and NAFLD/NASH progression, particularly with regard to liver fibrosis development, remains incompletely understood. We found that intermittent hypoxia could promote a pro-inflammatory and pro-fibrotic phenotype in our CDAA diet-fed animal model and increase circulating levels of EVs. Histological examination showed more portal inflammation in CDAA diet-fed mice exposed to IH compared with all the other groups. Interestingly, portal inflammation is considered a marker of severe disease in human NAFLD [66]. In our animal model, fibrosis, as determined by Sirius red staining, was significantly increased in CDAA diet-fed mice exposed to IH compared with the control groups. These results suggest that intermittent hypoxia can promote portal inflammation and fibrosis in an animal model of NASH and eventually fuel fibrogenesis. In line with this finding, a recent study demonstrated that accumulation of oxidized lipids, specifically low-density lipoproteins, in hepatocytes, promotes portal inflammation and fibrosis associated with progressive NAFLD [67]. With regard to the increase in circulating EVs, previous studies have demonstrated that IH mimicking OSA alters EV generation and release as well as EV-cargo and function, promoting pathophysiology in different *in vivo* models [67–69]. This important finding correlates with our *in vitro* results and provides evidence for a novel pro-fibrotic mechanism involving EVs. Future studies should address if circulating EVs are mostly derived from liver or from other specific cell sources. Also, full characterization of gene and protein cargoes contained in EVs as well as its precise membrane surface composition will be informative regarding signaling [...] d intercellular communications.

Among the limitations of the present study is the use of a chemical model of hypoxia instead of low oxygen-induced hypoxia. Although exposure of cells to a decreased oxygen concentration is the optimal hypoxia model, access to a hypoxia chamber or a CO_2 incubator with regulated oxygen levels is not always possible in many laboratories [38]. In the present study, the need for larger chambers to obtain sufficient media to isolate EVs also precluded the use of real hypoxia conditions. Of note, in addition to the differences in decreased oxygen concentration models, the $CoCl_2$-induced chemical hypoxia model is well accepted and provide stable experimental conditions that are informative regarding phenomena induced by real hypoxia [35,36,49]. Interestingly, a recent study from our laboratory using primary rat hepatocytes demonstrated that $CoCl_2$ mimicked the increase in HIF-1α expression observed under conditions of decreased oxygen concentrations without affecting cell viability [61]. Regardless, additional studies using real hypoxic conditions are desirable to confirm our findings and to better delineate the impact of hypoxia on the liver in the context of NASH, as well as the mechanisms underlying the hypoxia-induced release of EVs.

In conclusion, the present study showed that CoCl2 chemically induced hypoxia and intermittent hypoxia, promoted hepatocellular damage and increased pro-inflammatory and pro-fibrotic gene expression in hepatic cells that correlated with an increased release of EVs in both *in vitro* and in *in vivo* models of NAFLD/NASH. Moreover, EVs from fat-laden hepatic cells treated with CoCl2 evoked a pro-fibrotic response in LX-2 cells, suggesting a novel EV-mediated cell-to-cell communication in this model. Finally, mice fed a NASH-inducing diet and exposed to intermittent hypoxia exhibited a pro-inflammatory and pro-fibrotic phenotype that correlated with increases in circulating EVs. Future work should focus on profiling the genomic, transcriptomic, proteomic and lipidomic cargoes of EVs derived from liver cells under hypoxic conditions. Such information would help to identify hypoxia-specific molecules contributing to liver damage in NAFLD/NASH in the context of OSAS.

Supplementary data to this article can be found online at https://doi.org/10.1016/j.bbadis.2020.165857.

CRediT authorship contribution statement

Alejandra Hernández: Methodology, Investigation, Formal analysis, Writing - original draft.**Daniela Reyes:**Investigation, Formal analysis.**Yana Geng:**Methodology, Investigation, Formal analysis.**Juan Pablo Arab:**Investigation, Formal analysis.**Daniel Cabrera:**Investigation, Formal analysis.**Rolando Sepulveda**: Investigation, Formal analysis.**Nancy Solis:**Investigation, Formal analysis.**Manon Buist-Homan:**Investigation, Formal analysis.**Marco Arrese:**Methodology, Writing - original draft, Supervision, Funding acquisition.**Han Moshage:**Methodology, Writing - original draft, Supervision, Funding acquisition.

Declaration of competing interest

The authors declare that they have no known competing financial interests or personal relationships that could have appeared to influence the work reported in this paper.

References

[1] Z. Younossi, F. Tacke, M. Arrese, B. Chander Sharma, I. Mostafa, E. Bugianesi, V. Wai-Sun Wong, Y. Yilmaz, J. George, J. Fan, M.B. Vos, Global perspectives on nonalcoholic fatty liver disease and nonalcoholic steatohepatitis, Hepatology 69 (2019) 2672–2682.

[2] T.G. Cotter, M. Rinella, Nonalcoholic fatty liver disease 2020: the state of the disease, Gastroenterology 158 (2020) 1851–1864.

[3] J.P. Arab, M. Arrese, M. Trauner, Recent insights into the pathogenesis of non-alcoholic fatty liver disease, Annu. Rev. Pathol. 13 (2018) 321–350.

[4] M. Trauner, M. Arrese, M. Wagner, Fatty liver and lipotoxicity, Biochim. Biophys. Acta 1801 (2010) 299–310.

[5] S. Schuster, D. Cabrera, M. Arrese, A.E. Feldstein, Triggering and resolution of inflammation in NASH, Nat Rev Gastroenterol Hepatol 15 (2018) 349–364.

[6] M. Noureddin, A.J. Sanyal, Pathogenesis of NASH: the impact of multiple pathways, Curr Hepatol Rep 17 (2018) 350–360.

[7] K.E. Corey, R. Vuppalanchi, Assessment and management of comorbidities (including cardiovascular disease) in patients with nonalcoholic fatty liver disease, Clin Liver Dis (Hoboken) 1 (2012) 114–116.

[8] M. Arrese, F. Barrera, N. Triantafilo, J.P. Arab, Concurrent nonalcoholic fatty liver disease and type 2 diabetes: diagnostic and therapeutic considerations, Expert Rev Gastroenterol Hepatol 13 (2019) 849–866.

[9] S. Agrawal, A. Duseja, A. Das, M. Mehta, R.K. Dhiman, Y. Chawla, Obstructive sleep apnea is an important predictor of hepatic fibrosis in patients with nonalcoholic fatty liver disease in a tertiary care center, Hepatol. Int. 9 (2015) 283–291.

[10] O.A. Mesarwi, R. Loomba, A. Malhotra, Obstructive sleep apnea, hypoxia, and nonalcoholic fatty liver disease, Am. J. Respir. Crit. Care Med. 199 (2019) 830–841.

[11] K.J.P. Schwenger, Y. Ghorbani, C. Li, S.E. Fischer, T.D. Jackson, A. Okrainec, J.P. Allard, Obstructive sleep apnea and non-alcoholic fatty liver disease in obese patients undergoing bariatric surgery, Obes. Surg. 30 (2020) 2572–2578.

[12] J.A. Dempsey, S.C. Veasey, B.J. Morgan, C.P. O'Donnell, Pathophysiology of sleep apnea, Physiol. Rev. 90 (2010) 47–112.

[13] D.J. Gottlieb, N.M. Punjabi, Diagnosis and management of obstructive sleep apnea: a review, JAMA 323 (2020) 1389–1400.

[14] V. Savransky, S. Bevans, A. Nanayakkara, J. Li, P.L. Smith, M.S. Torbenson, V.Y. Polotsky, Chronic intermittent hypoxia causes hepatitis in a mouse model of diet-induced fatty liver, Am. J. Physiol. Gastrointest. Liver Physiol. 293 (2007) G871–G877.

[15] L.F. Drager, H.F. Lopes, C. Maki-Nunes, I.C. Trombetta, E. Toschi-Dias, M.J. Alves, R.F. Fraga, J.C. Jun, C.E. Negrao, E.M. Krieger, V.Y. Polotsky, G. Lorenzi-Filho, The impact of obstructive sleep apnea on metabolic and inflammatory markers in consecutive patients with metabolic syndrome, PLoS One 5 (2010) e12065.

[16] L.F. Drager, J. Li, C. Reinke, S. Bevans-Fonti, J.C. Jun, V.Y. Polotsky, Intermittent hypoxia exacerbates metabolic effects of diet-induced obesity, Obesity (Silver Spring) 19 (2011) 2167–2174.

[17] E. Paschetta, P. Belci, A. Alisi, D. Liccardo, R. Cutrera, G. Musso, V. Nobili, OSAS-related inflammatory mechanisms of liver injury in nonalcoholic fatty liver disease, Mediat. Inflamm. 2015 (2015) 815721.

[18] K. Nakayama, Cellular signal transduction of the hypoxia response, J. Biochem. 146 (2009) 757–765.

[19] Y. Liu, Z. Ma, C. Zhao, Y. Wang, G. Wu, J. Xiao, C.J. McClain, X. Li, W. Feng, HIF-1alpha and HIF-2alpha are critically involved in hypoxia-induced lipid accumulation in hepatocytes through reducing PGC-1alpha-mediated fatty acid beta-oxidation, Toxicol. Lett. 226 (2014) 117–123.

[20] O.A. Mesarwi, M.K. Shin, S. Bevans-Fonti, C. Schlesinger, J. Shaw, V.Y. Polotsky, Hepatocyte hypoxia inducible factor-1 mediates the development of liver fibrosis in a mouse model of nonalcoholic fatty liver disease, PLoS One 11 (2016) e0168572.

[21] A. Briancon-Marjollet, D. Monneret, M. Henri, M. Joyeux-Faure, P. Totoson, S. Cachot, P. Faure, D. Godin-Ribuot, Intermittent hypoxia in obese Zucker rats: cardiometabolic and inflammatory effects, Exp. Physiol. 101 (2016) 1432–1442.

[22] H.H. Kang, I.K. Kim, H.I. Lee, H. Joo, J.U. Lim, J. Lee, S.H. Lee, H.S. Moon, Chronic intermittent hypoxia induces liver fibrosis in mice with diet-induced obesity via TLR4/MyD88/MAPK/NF-kB signaling pathways, Biochem. Biophys. Res. Commun. 490 (2017) 349–355.

[23] W. Wu, W. Li, J. Wei, C. Wang, Y. Yao, W. Zhu, W. He, W. Zhou, J. Liu, Chronic intermittent hypoxia accelerates liver fibrosis in rats with combined hypoxia and nonalcoholic steatohepatitis via angiogenesis rather than endoplasmic reticulum stress, Acta Biochim. Biophys. Sin. Shanghai 51 (2019) 159–167.

[24] Y.F. Shi, C.C. Fong, Q. Zhang, P.Y. Cheung, C.H. Tzang, R.S. Wu, M. Yang, Hypoxia induces the activation of human hepatic stellate cells LX-2 through TGF-beta signaling pathway, FEBS Lett. 581 (2007) 203–210.

[25] B.L. Copple, J.J. Bustamante, T.P. Welch, N.D. Kim, J.O. Moon, Hypoxia-inducible factor-dependent production of profibrotic mediators by hypoxic hepatocytes, Liver Int. 29 (2009) 1010–1021.

[26] B.L. Copple, S. Bai, L.D. Burgoon, J.O. Moon, Hypoxia-inducible factor-1alpha regulates the expression of genes in hypoxic hepatic stellate cells important for collagen deposition and angiogenesis, Liver Int. 31 (2011) 230–244.

[27] D. Povero, A. Eguchi, H. Li, C.D. Johnson, B.G. Papouchado, A. Wree, K. Messer, A.E. Feldstein, Circulating extracellular vesicles with specific proteome and liver microRNAs are potential biomarkers for liver injury in experimental fatty liver disease, PLoS One 9 (2014) e113651.

[28] D. Povero, N. Panera, A. Eguchi, C.D. Johnson, B.G. Papouchado, L. de Araujo [...] Nobili, A.E. Feldstein, Lipid-induced hepatocyte [...] hepatic stellate cell via microRNAs targeting PPAR-gamma, Cell Mol Gastroenterol Hepatol 1 (2015) 646–663 (e644).

[29] P. Hirsova, S.H. Ibrahim, A. Krishnan, V.K. Verma, S.F. Bronk, N.W. Werneburg, M.R. Charlton, V.H. Shah, H. Malhi, G.J. Gores, Lipid-induced signaling causes release of inflammatory extracellular vesicles from hepatocytes, Gastroenterology 150 (2016) 956–967.

[30] S. Cannito, E. Morello, C. Bocca, B. Foglia, E. Benetti, E. Novo, F. Chiazza, M. Rogazzo, R. Fantozzi, D. Povero, S. Sutti, E. Bugianesi, A.E. Feldstein, E. Albano, M. Collino, M. Parola, Microvesicles released from fat-laden cells promote activation of hepatocellular NLRP3 inflammasome: a pro-inflammatory link between lipotoxicity and non-alcoholic steatohepatitis, PLoS One 12 (2017) e0172575.

[31] G. Szabo, F. Momen-Heravi, Extracellular vesicles in liver disease and potential as biomarkers and therapeutic targets, Nat Rev Gastroenterol Hepatol 14 (2017) 455–466.

[32] P.B. Devhare, R.B. Ray, Extracellular vesicles: novel mediator for cell to cell communications in liver pathogenesis, Mol. Asp. Med. 60 (2018) 115–122.

[33] A. Hernandez, J.P. Arab, D. Reyes, A. Lapitz, H. Moshage, J.M. Banales, M. Arrese, Extracellular vesicles in NAFLD/ALD: from pathobiology to therapy, Cells 9 (2020).

[34] A. Eguchi, A.E. Feldstein, Extracellular vesicles in non-alcoholic and alcoholic fatty liver diseases, Liver Res 2 (2018) 30–34.

[35] M. Pizarro, N. Solis, P. Quintero, F. Barrera, D. Cabrera, P. Rojas-de Santiago, J.P. Arab, O. Padilla, J.C. Roa, H. Moshage, A. Wree, E. Inzaugarat, A.E. Feldstein, C.E. Fardella, R. Baudrand, A. Riquelme, M. Arrese, Beneficial effects of mineralocorticoid receptor blockade in experimental non-alcoholic steatohepatitis, Liver Int. 35 (2015) 2129–2138.

[36] D. Cabrera, A. Wree, D. Povero, N. Solis, A. Hernandez, M. Pizarro, H. Moshage, J. Torres, A.E. Feldstein, C. Cabello-Verrugio, E. Brandan, F. Barrera, J.P. Arab, M. Arrese, Andrographolide ameliorates inflammation and fibrogenesis and attenuates inflammasome activation in experimental non-alcoholic steatohepatitis, Sci. Rep. 7 (2017) 3491.

[37] N.C. Chavez-Tapia, N. Rosso, C. Tiribelli, In vitro models for the study of non-alcoholic fatty liver disease, Curr. Med. Chem. 18 (2011) 1079–1084.

[38] J. Munoz-Sanchez, M.E. Chanez-Cardenas, The use of cobalt chloride as a chemical hypoxia model, J. Appl. Toxicol. 39 (2019) 556–570.

[39] M. Pecoraro, A. Pinto, A. Popolo, Inhibition of Connexin 43 translocation on mitochondria accelerates CoCl2-induced apoptotic response in a chemical model of hypoxia, Toxicol. in Vitro 47 (2018) 120–128.

[40] M.H. Schoemaker, L. Conde de la Rosa, M. Buist-Homan, T.E. Vrenken, R. Havinga, K. Poelstra, H.J. Haisma, P.L. Jansen, H. Moshage, Tauroursodeoxycholic acid protects rat hepatocytes from bile acid-induced apoptosis via activation of survival pathways, Hepatology 39 (2004) 1563–1573.

[41] L.L. Chan, K.J. McCulley, S.L. Kessel, Assessment of cell viability with single-, dual-, and multi-staining methods using image cytometry, Methods Mol Biol 1601 (2017) 27–41.

[42] C. Thery, S. Amigorena, G. Raposo, A. Clayton, Isolation and characterization of exosomes from cell culture supernatants and biological fluids, Curr Protoc Cell Biol Chapter 3 (Unit 3) (2006) 22.

[43] L. Xu, A.Y. Hui, E. Albanis, M.J. Arthur, S.M. O'Byrne, W.S. Blaner, P. Mukherjee, S.L. Friedman, F.J. Eng, Human hepatic stellate cell lines, LX-1 and LX-2: new tools for analysis of hepatic fibrosis, Gut 54 (2005) 142–151.

[44] A.E. Feldstein, A. Canbay, M.E. Guicciardi, H. Higuchi, S.F. Bronk, G.J. Gores, Diet associated hepatic steatosis sensitizes to Fas mediated liver injury in mice, J. Hepatol. 39 (2003) 978–983.

[45] C. Thery, K.W. Witwer, E. Aikawa, M.J. Alcaraz, J.D. Anderson, R. Andriantsitohaina, A. Antoniou, T. Arab, F. Archer, G.K. Atkin-Smith, D.C. Ayre, J. M. Bach, D. Bachurski, H. Baharvand, L. Balaj, S. Baldacchino, N.N. Bauer, A.A. Baxter, M. Bebawy, C. Beckham, A. Bedina Zavec, A. Benmoussa, A.C. Berardi, P. Bergese, E. Bielska, C. Blenkiron, S. Bobis-Wozowicz, E. Boilard, W. Boireau, A. Bongiovanni, F.E. Borras, S. Bosch, C.M. Boulanger, X. Breakefield, A.M. Breglio, M. A. Brennan, D.R. Brigstock, A. Brisson, M.L. Broekman, J.F. Bromberg, P. Bryl-Gorecka, S. Buch, A.H. Buck, D. Burger, S. Busatto, D. Buschmann, B. Bussolati, E.I. Buzas, J.B. Byrd, G. Camussi, D.R. Carter, S. Caruso, L.W. Chamley, Y.T. Chang, C. Chen, S. Chen, L. Cheng, S.K. Chin, A. Clayton, S.P. Clerici, A. Cocks, E. Cocucci, R. J. Coffey, A. Cordeiro-da-Silva, Y. Couch, F.A. Coumans, B. Coyle, R. Crescitelli, M. F. Criado, C. D'Souza-Schorey, S. Das, A. Datta Chaudhuri, P. de Candia, E.F. De Santana, O. De Wever, H.A. Del Portillo, T. Demaret, S. Deville, A. Devitt, B. Dhondt, D. Di Vizio, L.C. Dieterich, V. Dolo, A.P. Dominguez Rubio, M. Dominici, M.R. Dourado, T.A. Driedonks, F.V. Duarte, H.M. Duncan, R.M. Eichenberger, K. Ekstrom, S. El Andaloussi, C. Elie-Caille, U. Erdbrugger, J.M. Falcon-Perez, F. Fatima, J.E. Fish, M. Flores-Bellver, A. Forsonits, A. Frelet-Barrand, F. Fricke, G. Fuhrmann, S. Gabrielsson, A. Gamez-Valero, C. Gardiner, K. Gartner, R. Gaudin, Y. S. Gho, B. Giebel, C. Gilbert, M. Gimona, I. Giusti, D.C. Goberdhan, A. Gorgens, S.M. Gorski, D.W. Greening, J.C. Gross, A. Gualerzi, G.N. Gupta, D. Gustafson, A. Handberg, R.A. Haraszti, P. Harrison, H. Hegyesi, A. Hendrix, A.F. Hill, F.H. Hochberg, K.F. Hoffmann, B. Holder, H. Holthofer, B. Hosseinkhani, G. Hu, Y. Huang, V. Huber, S. Hunt, A.G. Ibrahim, T. Ikezu, J.M. Inal, M. Isin, A. Ivanova, H. K. Jackson, S. Jacobsen, S.M. Jay, M. Jayachandran, G. Jenster, L. Jiang, S.M. Johnson, J.C. Jones, A. Jong, T. Jovanovic-Talisman, S. Jung, R. Kalluri, S.I. Kano, S. Kaur, Y. Kawamura, E.T. Keller, D. Khamari, E. Khomyakova, A. Khvorova, P. Kierulf, K.P. Kim, T. Kislinger, M. Klingeborn, D.J. Klinke, 2nd, M. Kornek, M.M. Kosanovic, A.F. Kovacs, E.M. Kramer-Albers, S. Krasemann, M. Krause, I.V. Kurochkin, G.D. Kusuma, S. Kuypers, S. Laitinen, S.M. Langevin, L.R. Languino, J. Lannigan, C. Lasser, L.C. Laurent, G. Lavieu, E. Lazaro-Ibanez, S. Le Lay, M.S. Lee, Y. X.F. Lee, D.S. Lemos, M. Lenassi, A. Leszczynska, I.T. Li, K. Liao, S.F. Libregts, E. Ligeti, R. Lim, S.K. Lim, A. Line, K. Linnemannstons, A. Llorente, C.A. Lombard, M. J. Lorenowicz, A.M. Lorincz, J. Lotvall, J. Lovett, M.C. Lowry, X. Loyer, Q. Lu, B. Lukomska, T.R. Lunavat, S.L. Maas, H. Malhi, A. Marcilla, J. Mariani, J. Mariscal, E.

S. Martens-Uzunova, L. Martin-Jaular, M.C. Martinez, V.R. Martins, M. Mathieu, S. Mathivanan, M. Maugeri, L.K. McGinnis, M.J. McVey, D.G. Meckes, Jr., K.L. Meehan, I. Mertens, V.R. Minciacchi, A. Moller, M. Moller Jorgensen, A. Morales-Kastresana, J. Morhayim, F. Mullier, M. Muraca, L. Musante, V. Mussack, D.C. Muth, K.H. Myburgh, T. Najrana, M. Nawaz, I. Nazarenko, P. Nejsum, C. Neri, T. Neri, R. Nieuwland, L. Nimrichter, J.P. Nolan, E.N. Nolt-e't Hoen, N. Noren Hooten, L. O'Driscoll, T. O'Grady, A. O'Loghlen, T. Ochiya, M. Olivier, A. Ortiz, L.A. Ortiz, X. Osteikoetxea, O. Ostergaard, M. Ostrowski, J. Park, D.M. Pegtel, H. Peinado, F. Perut, M.W. Pfaffl, D.G. Phinney, B.C. Pieters, R.C. Pink, D.S. Pisetsky, E. Pogge von Strandmann, I. Polakovicova, I.K. Poon, B.H. Powell, I. Prada, L. Pulliam, P. Quesenberry, A. Radeghieri, R.L. Raffai, S. Raimondo, J. Rak, M.I. Ramirez, G. Raposo, M.S. Rayyan, N. Regev-Rudzki, F.L. Ricklefs, P.D. Robbins, D.D. Roberts, S. C. Rodrigues, E. Rohde, S. Rome, K.M. Rouschop, A. Rughetti, A.E. Russell, P. Saa, S. Sahoo, E. Salas-Huenuleo, C. Sanchez, J.A. Saugstad, R.M. Schiffelers, R. Schneider, T.H. Schoyen, A. Scott, E. Shahaj, S. Sharma, O. Shatnyeva, F. Shekari, G.V. Shelke, A.K. Shetty, K. Shiba, P.R. Siljander, A.M. Silva, A. Skowronek, O.L. Snyder, 2nd, R.P. Soares, B.W. Sodar, C. Soekmadji, J. Sotillo, P.D. Stahl, W. Stoorvogel, S.L. Stott, E.F. Strasser, S. Swift, H. Tahara, M. Tewari, K. Timms, S. Tiwari, R. Tixeira, M. Tkach, W.S. Toh, R. Tomasini, A.C. Torrecilhas, J.P. Tosar, V. Toxavidis, L. Urbanelli, P. Vader, B.W. van Balkom, S.G. van der Grein, J. Van Deun, M.J. van Herwijnen, K. Van Keuren-Jensen, G. van Niel, M.E. van Royen, A.J. van Wijnen, M.H. Vasconcelos, I.J. Vechetti, Jr., T.D. Veit, L.J. Vella, E. Velot, F.J. Verweij, B. Vestad, J.L. Vinas, T. Visnovitz, K.V. Vukman, J. Wahlgren, D.C. Watson, M.H. Wauben, A. Weaver, J.P. Webber, V. Weber, A.M. Wehman, D.J. Weiss, J.A. Welsh, S. Wendt, A.M. Wheelock, Z. Wiener, L. Witte, J. Wolfram, A. Xagorari, P. Xander, J. Xu, X. Yan, M. Yanez-Mo, H. Yin, Y. Yuana, V. Zappulli, J. Zarubova, V. Zekas, J.Y. Zhang, Z. Zhao, L. Zheng, A.R. Zheutlin, A.M. Zickler, P. Zimmermann, A.M. Zivkovic, D. Zocco, E.K. Zuba-Surma, Minimal information for studies of extracellular vesicles 2018 (MISEV2018): a position statement of the International Society for Extracellular Vesicles and update of the MISEV2014 guidelines, J Extracell Vesicles, 7 (2018) 1535750.

[46] E. Vilar-Gomez, L. Calzadilla-Bertot, V. Wai-Sun Wong, M. Castellanos, R. Aller-de la Fuente, M. Metwally, M. Eslam, L. Gonzalez-Fabian, M. Alvarez-Quinones Sanz, A.F. Conde-Martin, B. De Boer, D. McLeod, A.W. Hung Chan, N. Chalasani, J. George, L.A. Adams, M. Romero-Gomez, Fibrosis severity as a determinant of cause-specific mortality in patients with advanced nonalcoholic fatty liver disease: a multi-national cohort study, Gastroenterology 155 (2018) 443–457 (e417).

[47] O.A. Mesarwi, M.K. Shin, L.F. Drager, S. Bevans-Fonti, J.C. Jun, N. Putcha, M.S. Torbenson, R.P. Pedrosa, G. Lorenzi-Filho, K.E. Steele, M.A. Schweitzer, T.H. Magnuson, A.O. Lidor, A.R. Schwartz, V.Y. Polotsky, Lysyl oxidase as a serum biomarker of liver fibrosis in patients with severe obesity and obstructive sleep apnea, Sleep 38 (2015) 1583–1591.

[48] M. Buttacavoli, C.I. Gruttad'Auria, M. Olivo, R. Virdone, A. Castrogiovanni, E. Mazzuca, A.M. Marotta, O. Marrone, S. Madonia, M.R. Bonsignore, Liver Steatosis and fibrosis in OSA patients after long-term CPAP treatment: a preliminary ultrasound study, Ultrasound Med. Biol. 42 (2016) 104–109.

[49] S.Z. Feng, J.L. Tian, Q. Zhang, H. Wang, N. Sun, Y. Zhang, B.Y. Chen, An experimental research on chronic intermittent hypoxia leading to liver injury, Sleep Breath. 15 (2011) 493–502.

[50] S.L. Friedman, B.A. Neuschwander-Tetri, M. Rinella, A.J. Sanyal, Mechanisms of NAFLD development and therapeutic strategies, Nat. Med. 24 (2018) 908–922.

[51] S.L. Friedman, Hepatic stellate cells: protean, multifunctional, and enigmatic cells of the liver, Physiol. Rev. 88 (2008) 125–172.

[52] Y.J. Jeon, K.S. Song, H.J. Han, S.H. Park, W. Chang, M.Y. Lee, Rosmarinic acid inhibits chemical hypoxia-induced cytotoxicity in primary cultured rat hepatocytes, Arch. Pharm. Res. 37 (2014) 907–915.

[53] J.J.G. Marin, E. Lozano, M.J. Perez, Lack of mitochondrial DNA impairs chemical hypoxia-induced autophagy in liver tumor cells through ROS-AMPK-ULK1 signaling dysregulation independently of HIF-1alpha, Free Radic. Biol. Med. 101 (2016) 71–84.

[54] M. Ricchi, M.R. Odoardi, L. Carulli, C. Anzivino, S. Ballestri, A. Pinetti, L.I. Fantoni, F. Marra, M. Bertolotti, S. Banni, A. Lonardo, N. Carulli, P. Loria, Differential effect of oleic and palmitic acid on lipid accumulation and apoptosis in cultured hepatocytes, J. Gastroenterol. Hepatol. 24 (2009) 830–840.

[55] A. Moravcova, Z. Cervinkova, O. Kucera, V. Mezera, D. Rychtrmoc, H. Lotkova, The effect of oleic and palmitic acid on induction of steatosis and cytotoxicity on rat hepatocytes in primary culture, Physiol. Res. 64 (Suppl. 5) (2015) S627–S636.

[56] J. Li, L.N. Thorne, N.M. Punjabi, C.K. Sun, A.R. Schwartz, P.L. Smith, R.L. Marino, A. Rodriguez, W.C. Hubbard, C.P. O'Donnell, V.Y. Polotsky, Intermittent hypoxia induces hyperlipidemia in lean mice, Circ. Res. 97 (2005) 698–706.

[57] X. Chen, L. Li, X. Liu, R. Luo, G. Liao, L. Li, J. Liu, J. Cheng, Y. Lu, Y. Chen, Oleic acid protects saturated fatty acid mediated lipotoxicity in hepatocytes and rat of non-alcoholic steatohepatitis, Life Sci. 203 (2018) 291–304.

[58] A.E. Feldstein, N.W. Werneburg, A. Canbay, M.E. Guicciardi, S.F. Bronk, R. Rydzewski, L.J. Burgart, G.J. Gores, Free fatty acids promote hepatic lipotoxicity by stimulating TNF-alpha expression via a lysosomal pathway, Hepatology 40 (2004) 185–194.

[59] H. Malhi, G.J. Gores, J.J. Lemasters, Apoptosis and necrosis in the liver: a tale of two deaths? Hepatology 43 (2006) S31–S44.

[60] A. Payance, G. Silva-Junior, J. Bissonnette, M. Tanguy, B. Pasquet, C. Levi, O. Roux, O. Nekachtali, A. Baiges, V. Hernandez-Gea, C. Laouenan, D. Lebrec, M. Albuquerque, V. Paradis, R. Moreau, D. Valla, F. Durand, C.M. Boulanger, J.C. Garcia-Pagan, P.E. Rautou, Hepatocyte microvesicle levels improve prediction of mortality in patients with cirrhosis, Hepatology 68 (2018) 1508–1518.

[61] F. Momen-Heravi, S. Bala, K. Kodys, G. Szabo, Exosomes derived from alcohol-treated hepatocytes horizontally transfer liver specific miRNA-122 and sensitize monocytes to LPS, Sci. Rep. 5 (2015) 9991.

[62] Y.S. Lee, S.Y. Kim, E. Ko, J.H. Lee, H.S. Yi, Y.J. Yoo, J. Je, S.J. Suh, Y.K. Jung, J.H. Kim, Y.S. Seo, H.J. Yim, W.I. Jeong, J.E. Yeon, S.H. Um, K.S. Byun, Exosomes derived from palmitic acid-treated hepatocytes induce fibrotic activation of hepatic stellate cells, Sci. Rep. 7 (2017) 3710.

[63] D. Povero, A. Eguchi, I.R. Niesman, N. Andronikou, X. de Mollerat du Jeu, A. Mulya, M. Berk, M. Lazic, S. Thapaliya, M. Parola, H.H. Patel, A.E. Feldstein, Lipid-induced toxicity stimulates hepatocytes to release angiogenic microparticles that require Vanin-1 for uptake by endothelial cells, Sci Signal 6 (2013) ra88.

[64] A. Hernandez, Y. Geng, R. Sepulveda, N. Solis, J. Torres, J.P. Arab, F. Barrera, D. Cabrera, H. Moshage, M. Arrese, Chemical hypoxia induces pro-inflammatory signals in fat-laden hepatocytes and contributes to cellular crosstalk with Kupffer cells through extracellular vesicles, Biochim. Biophys. Acta Mol. basis Dis. 2020 (1866) 165753.

[65] I. Almendros, Y. Wang, L. Becker, F.E. Lennon, J. Zheng, B.R. Coats, K.S. Schoenfelt, A. Carreras, F. Hakim, S.X. Zhang, R. Farre, D. Gozal, Intermittent hypoxia-induced changes in tumor-associated macrophages and tumor malignancy in a mouse model of sleep apnea, Am. J. Respir. Crit. Care Med. 189 (2014) 593–601.

[66] E.M. Brunt, D.E. Kleiner, L.A. Wilson, A. Unalp, C.E. Behling, J.E. Lavine, B.A. Neuschwander-Tetri, N.C.R.N.l.o.m.o.t.N.S.C.R.N.c.b.f.i.t. Appendix, Portal chronic inflammation in nonalcoholic fatty liver disease (NAFLD): a histologic marker of advanced NAFLD-Clinicopathologic correlations from the nonalcoholic steatohepatitis clinical research network, Hepatology, 49 (2009) 809–820.

[67] C.M. Ho, S.L. Ho, Y.M. Jeng, Y.S. Lai, Y.H. Chen, S.C. Lu, H.L. Chen, P.Y. Chang, R.H. Hu, P.H. Lee, Accumulation of free cholesterol and oxidized low-density lipoprotein is associated with portal inflammation and fibrosis in nonalcoholic fatty liver disease, J Inflamm (Lond) 16 (2019) 7.

[68] Y. Luo, H.Y. Dong, B. Zhang, Z. Feng, Y. Liu, Y.Q. Gao, M.Q. Dong, Z.C. Li, miR-29a-3p attenuates hypoxic pulmonary hypertension by inhibiting pulmonary adventitial fibroblast activation, Hypertension 65 (2015) 414–420.

[69] A. Khalyfa, R. Cortese, Z. Qiao, H. Ye, R. Bao, J. Andrade, D. Gozal, Late gestational intermittent hypoxia induces metabolic and epigenetic changes in male adult offspring mice, J. Physiol. 595 (2017) 2551–2568.